Review

Ikrame Najihi*, Chouaib Ennawaoui, Abdelowahed Hajjaji and Yahia Boughaleb

Exploring the piezoelectric porous polymers for energy harvesting: a review

https://doi.org/10.1515/ehs-2022-0159
Received November 28, 2022; accepted May 14, 2023;
published online June 5, 2023

Abstract: In addition to traditional piezoelectric polymers, mono-crystals and ceramics, piezoelectrets or charged voided polymers have shown an interesting piezoelectric response by converting the mechanical energy into electrical and vice versa, therefore being incorporated in a number of advanced electromechanical transducers. This article is a review on the different phases for the elaboration of pseudo piezoelectric films based on passive polymers. First, several methods for the elaboration of the cellular structure of these materials are explained in the main text, with the morphological representation of the reached porosity. The porosity represents a cell to embed the positive and negative electrical charges created by the most common electrical charging processes, which are subsequently mentioned. Different theoretical models are emphasized as well to predict the piezoelectric behavior of this porous polymers. Finally, some of the latest harvesting energy applications based on porous polymers are collected. All the considerations cited above make Piezoelectric porous polymers open access materials that can be developed and optimized by the control of the porosity then used in energy harvesting applications.

***Corresponding author: Ikrame Najihi**, Laboratory of Engineering Sciences for Energy, National School of Applied Sciences, Chouaib Doukkali University, El Jadida, Morocco, E-mail: najihi.ikram@gmail.com. https://orcid.org/0000-0002-7059-0128
Chouaib Ennawaoui, Laboratory of Engineering Sciences for Energy, National School of Applied Sciences, Chouaib Doukkali University, El Jadida, Morocco; and Green Tech Institute (GTI), Mohammed VI Polytechnic University (UM6P), Benguerir, Morocco
Abdelowahed Hajjaji, Laboratory of Engineering Sciences for Energy, National School of Applied Sciences, Chouaib Doukkali University, El Jadida, Morocco; and High School of Education and Training, Chouaib Doukkali University, El Jadida, Morocco
Yahia Boughaleb, Laboratory of Condensed Matter Physics, Faculty of Science, Chouaib Doukkali University, El Jadida, Morocco; and Bio-Geosciences and Materials Engineering Laboratory, Ecole Normale Supérieure, University Hassan II, Casablanca, Morocco

Keywords: electrets; energy harvesting; piezoelectricity; porous polymers.

1 Introduction

Facing the energy crisis, research has been mobilized to find alternative energy sources and harvest ambient energy, in order to supply power and make small devices energetically autonomous. A new solution to this issue is the piezoelectric energy harvesters that use the wasted energy from their surroundings through the piezoelectric effect, which is the ability of certain materials to generate electricity when they are subjected to a mechanical stress.

The phenomenon of piezoelectricity was first observed in 1817 by René Just Haüy then discovered by the brothers Pierre and Jacques Curie, who predicted the existence of piezoelectricity on quartz crystals, discovered the phenomenon in 1880 (Mason 1981). One year later, the opposite effect was predicted by Gabriel Lippmann and was verified by the Curie brothers. Woldemar Voigt, a German physicist who presents the twenty piezoelectric crystal classes, gathered all the theoretical work on piezoelectricity in 1918 in the Manual of Crystal Physics. The piezoelectric effect can occur in all directions and be divided in two main effects as seen in Figure 1. The direct piezoelectric effect corresponds to the production of electrical charges under mechanical stress, and the inverse piezoelectric effect associated to the deformation of a material when subjected to an electric field.

The piezoelectric effect is found in crystalline materials with an asymmetric atomic structure, where an electric dipole is created after deformation (Senturia 2007), also in ferroelectric materials (Setter et al. 2006), which in the spontaneous state have an electric polarization that can be reoriented by the application of an external electric field. The ferroelectric materials are made of several small (self-assembling) ferroelectric domains that are randomly oriented. Under the effect of a sufficiently strong external electric field, these ferroelectric domains align in the same direction as the field and there is then spontaneous polarization.

There are three main categories of piezoelectric materials: crystals and ceramics which, by nature, have an

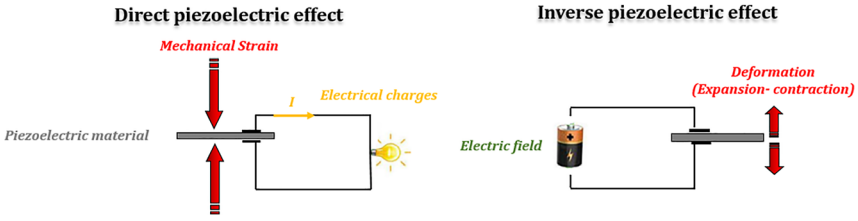

Figure 1: The main piezoelectric effects.

excellent piezoelectric response (Song et al. 2017), and have shown their ability to harvest a significant amount of energy (Fangachi et al. 2022; Malki et al. 2020). The third category consists of piezoelectric polymers which have the advantages of being lightweight, low cost, highly flexible and thin (Ham et al. 2021; Won et al. 2020). However, they have shown a relatively weak piezoelectric coefficient d_{33} compared to ceramics (Lopes et al. 2011; Zhong et al. 2017). Therefore, the need for polymer-based materials with good piezoelectric performance led to the development of piezoelectric cellular polymers called piezoelectret, with internal charged voids that serve as artificial dipoles.

Polymers with a porous structure were created with the aim of developing new materials having a higher piezoelectric power and a wide range of mechanical, thermal and electrical properties while lowering production costs. Piezo-cellular materials have emerged as a new alternative to ceramics and piezoelectric single crystals (Lanceros-Méndez and Martins 2017). Piezoelectricity in these materials is not based on their intrinsic properties, but on the elaboration process, that gives the materials the piezoelectric character by holding the macro-dipoles in the voids of the film (Gerhard-Multhaupt and Less 2002). The elaboration process of piezo-cellular films must be well-precise in order to develop a voided structure with a non-interconnected porosity and a good morphology, where each void serves as a macro-dipole charged in the direction of the thickness of the polymer film. Then, the electrical charging ionizes the gas inside the pores and activates the piezoelectric character. These processes will be enlightened in the following sections as techniques reviewed in the literature.

2 Voided structure elaboration

Porous polymers are obtained from synthetic polymers of olefinic monomers (or alkenes, i.e. unsaturated hydrocarbons C_nH_{2n} with one or more carbon-carbon bonds) (Yasuda and Lamaze 1973). They can be classified by monomer unit and chain structure: polyolefin-based ethylene, polyolefin-based propylene and polyolefin-based elastomers (Wang et al. 2019). They can also be categorized according to the interne structure; open cell or closed cell foams. Then again, depending on the density; very light, light, medium, heavy and very heavy. Their use is widespread due to their semi-crystalline thermoplastic nature, their inertia with various chemical agents and their crystallinity degree of about 30 % (Kong and Hay 2002). They have electrical advantages, owing to their high resistivity and particular cellular structure that holds electrical charges (Warfield and Petree 1961).

When foaming a plastic material, the solid melts under temperature then internal voids are homogenously created by the injection of a gas or the intervention of a chemical/solid particles and finally it solidifies and stabilizes. The widely used foaming process for thermoplastics is the gas dispersion through a fluid polymer. The gases used to foam could come from different sources. For example the air forced into a fluid plastic (De Vries 2009), the carbon dioxide (CO_2) embedded in a plastic under pressure (Fang et al. 2007), Low boiling liquid dissolved in a polymer then changed into a gas by undergoing temperature or compression or gases produced by a chemical reaction decomposition (i.e. the azodicarbonamide ($C_2H_4O_2N_4$ known as E927)) (Samadi et al. 2020).

During the foaming process, the early bubbles may grow by gas diffusion into the molten mixture (Wegener et al. 2004), mechanical extension of these bubbles (Qaiss and Bousmina 2011), temperature, compression or by combination of two or more bubbles (Stevenson 2010). If the cell membranes surrounding a bubble remain undamaged, foams are called closed cell foams. If these membranes

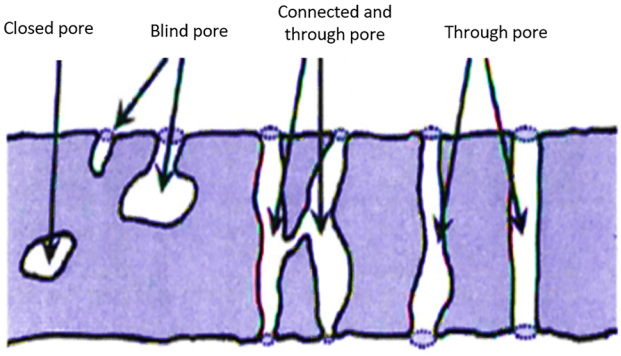

Figure 2: Types of cells.

are broken, they are called open cells. Figure 2 shows the differences between closed and open cells (Konstantinidis, Paradisiadis, and Tsipas 2009).

3 Cellular film production techniques

3.1 Stretched film with fillers technique

The production process of cellular films can be achieved by the incorporation of different kinds of filler particles then the stretching or the inflation of the obtained films (Audet et al. 2018; Kaczmarek et al. 2019; Klimiec et al. 2020a). An experimental study was explained in Figure 3, where Hillenbrand et al. (2006) subjected polymer films, filled with micro particles, to a uniaxial stretching. The cellular Polypropylene films were produced by feeding an extruder with polypropylene powder and three micro particles; the nucleating agent 2,2-methylene-bis-(4,6-di-tert-butylphenyl)-phosphate (NA_{11}), calcium carbonate ($CaCO_3$) and alumina (Al_2O_3). Where the effect of different concentrations of each filler on the charge stability was investigated. The fillers must have low chemical bonding affinities with the polymer so that it does not attach to it. The interfacial decohesion permit the creation of micro-cracks around the filler particles that will expand into pores while stretching. After the extrusion of a 300 µm thick film, five layers of the film were subjected to hot pressure to obtain a multilayer film with a thickness of less than 1 mm. Finally, it was stretched at a temperature of 155 °C.

This technique allows the creation of very long, stretched and non-interconnected cells, as well as the improvement of the charge stability of the porous polymer owing to inorganic additives.

3.2 Thermo-forming template technique

Recently, methods are being developed to produce well-defined pores in polymer films based on the template forming technique in different fields (Yan et al. 2004). This technique consist on applying a heat source on a template and an odd of different layers stacked alternately (Zhang, Hillenbrand, and Sessler 2007). In the following study, Zhang, Hillenbrand, and Sessler (2006) used three polymer layer, the Polytetrafluoroethylene (PTFE) polymer-based middle layer that is characterized by a relatively low melting temperature and will melt and bond the outer layers based on Fluoroethylenepropylene (FEP). The pressing by template ensures precision in cell shape and size. It gives better results in terms of cell homogeneity compared to other techniques but with poor surface quality. Figure 4 shows the shape of the obtained cells and the rigorous appearance at the film surface.

Another technique consists in inserting a 100 µm thick polytetrafluoroethylene film, containing parallel rectangles holes, between two 50 µm thick fluoroethylenepropylene films (Altafim et al. 2009). The films were then hot-pressed at a temperature of 300 °C and so the FEP films were adhered together through the openings of the rectangles. Then finally, the PTFE film was removed, leaving a tubular structure in the PEF film (see Figure 5).

In Figure 6, Altafim et al. used a special mechanical configuration to thermo-form a regular network of cells between two polymer films (Altafim et al. 2006). The experimental setup consists of two cylindrical metal parts that were heated independently and a metal grid in the middle. The upper part is a solid electric heating system, while the lower part is connected to a vacuum pump and has twenty holes for suction. The sample, which is two fluoroethylenepropylene films, is placed between the heating parts and the grid, which is in turn placed on the lower part. Once the vacuum pump is activated, both films are

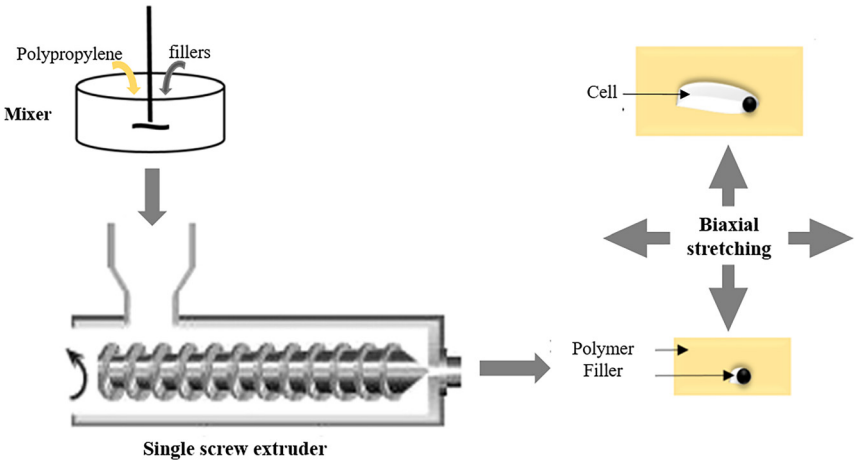

Figure 3: Cell creation by the micro particle injection method.

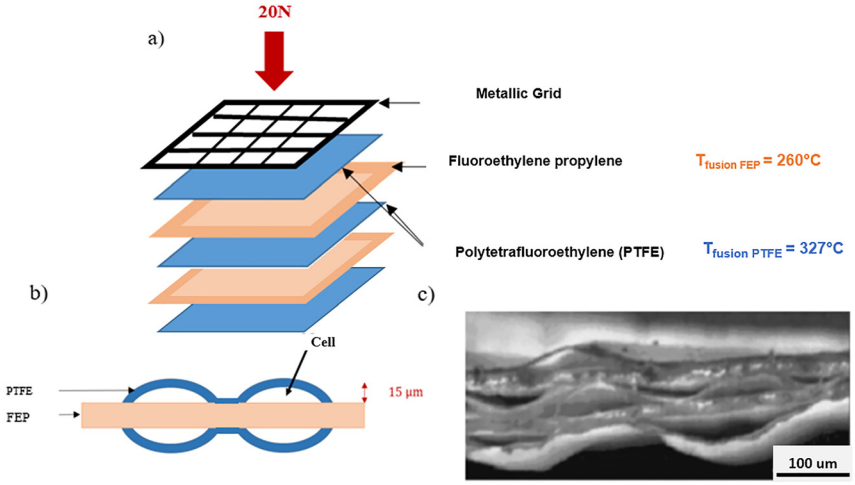

Figure 4: Thermo-forming technique, (a) exerimental setup, (b) the obtained porosity, and (c) the cross-section view scanning electron microscope (SEM).

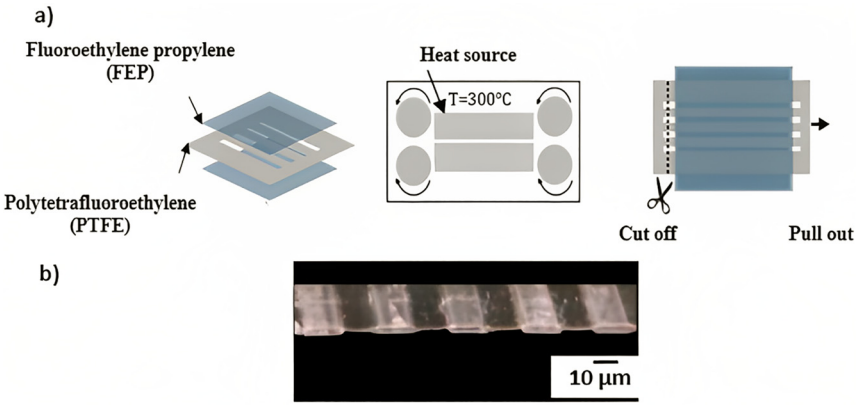

Figure 5: The elaboration process of the tubular structure, (a) the process, and (b) the optical micrograph of the cross section of the film surface.

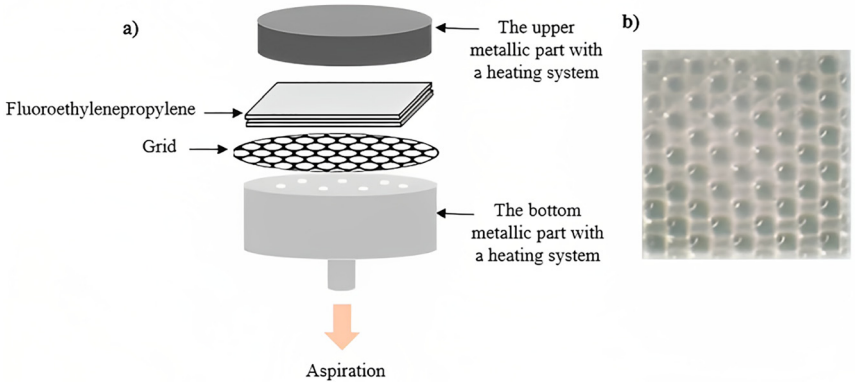

Figure 6: FEP cellular film, (a) experimental setup of thermo-formed cells, and (b) the created air bubble (Altafim et al. 2006).

sucked into the overtures of the grille. As soon as the upper metal part is heated to about 200 °C and pressed onto the films, air cells of the same diameter as the grid openings are created. Another similar study consists in pre-molding one Teflon FEP film into a dome shape bubbles by the application of a hydraulic press, then bonding it to another Teflon FEP single film by hot lamination process (Falconi et al. 2010).

These last two techniques have the disadvantage of the roughness of the surface condition, which subsequently causes a problem in terms of electrode deposition on the surfaces.

3.3 High-pressure foaming technique in supercritical CO_2

A supercritical fluid is a product with a pressure and temperature above their critical values. It possesses properties intermediate between those of gases and liquids. The potential of gas molecules to diffuse into the polymer mass reveals a further technique for foaming process in general (Fang et al. 2007; Han et al. 2003; Japon, Leterrier, and Månson 2000; Moghadam et al. 2017). For the production of piezoelectric porous polymer many films were established by means of this technique (Wirges et al. 2007) which is based on the treatment of polymers at high pressure in the presence of supercritical gas (usually N_2 or CO_2) that diffuses easily into polymers and changes the rheological properties of the material by playing the role of an expansion agent. The diffusion of gas molecules depends not only on the properties of the matrix but also on the pressure, the temperature and the time of elaboration process. The size of the obtained porosity ranges from micrometers to nanometers depending on the operating parameters of the treatments.

In general, with supercritical gases, porous polymer films can be obtained by following the same steps with the possibility of modifying the operating parameters. Figure 7 summarizes the steps required for the preparation of porous poly(ethylene terephthalate) (PETP) film under supercritical CO_2 (Wirges et al. 2007). First, a non-porous sample is exposed to supercritical carbon dioxide CO_2 in a pressure chamber at 100 bar. Then, the sample undergoes a thermal treatment above the glass-transition temperature that leads to a volume increase of the trapped CO_2 and consequently to the creation of spherical voids inside the polymer matrix film. Finally, for the dimensional adjustment of the obtained porosity, the film was subjected to a successive biaxial stretching following by an inflation by means of gas diffusion under N_2. The time of the gas-pressure treatment, the heat treatment and the inflation was varied to investigate how this affect the density in general and the void size in particular. The scanning electron microscope illustrates a major disadvantage of the technique, which is the interconnection of cells during creation that subsequently influences the activation of the piezoelectric effect; however, this technique does not cause any pollution problem.

3.4 Hybrid technique with bi-axial stretching and gas injection

In order to create a piezo cellular film, Qaiss et all used a hybrid technique that combines the filler technique, the biaxial stretching and pressurized gas inflation using a home-developed devices (Qaiss et al. 2012). Figure 8 shows the cellular morphology done by a scanning electron microscopy and summarizes the three steps of the hybrid technique that starts with the extrusion of a mixture of Polypropylene and $CaCO_3$ microparticles, followed by a bi-axial stretching and N_2 gas diffusion swelling of the output film with home-developed devices (Qaiss and Bousmina 2011) (see Figure 9).

3.5 Three-dimensional printing technique

The three-dimensional printing or additive manufacturing (AM) is an important process for prototyping that helps in fast and accurate manufacturing with reducing material consumption and processing safe. Like a traditional printer, the 3D printer is a computer-aided manufacturing device that creates objects from digital data as input. However, instead of printing ink on paper, it use raw materials to build layer by layer a three-dimensional model. The materials used by current 3D printers are polymers, metals, concrete and ceramic material that were used in the construction

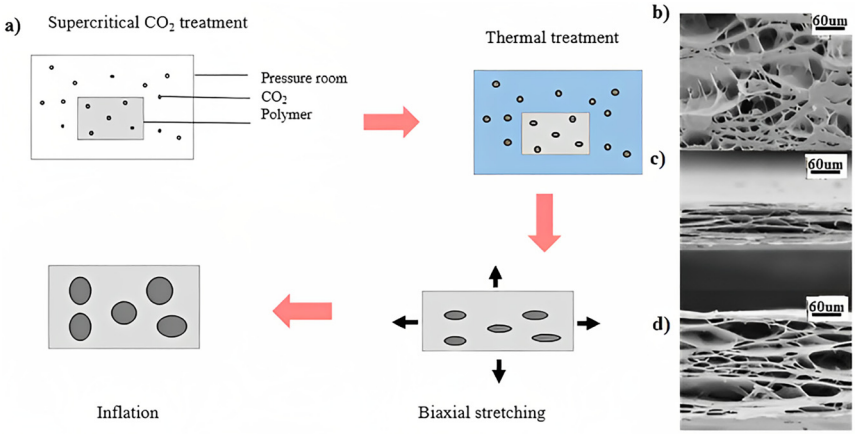

Figure 7: High pressure treatment in the presence of supercritical CO_2, (a) the porosity creation process (b) a scanning Electron Microscopy image of the foam structure after each step (Wirges et al. 2007).

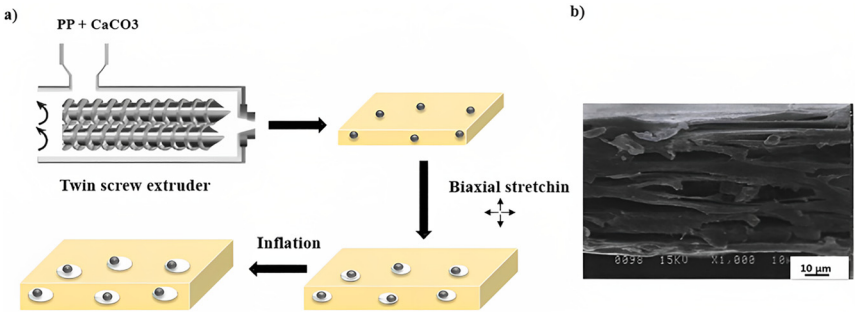

Figure 8: Biaxial stretching of filled film, (a) principle of the hybrid technique and (b) the scanning electron microscopy image (SEM) of the stretched PP-$CaCO_3$ film filled with 10% of $CaCO_3$.

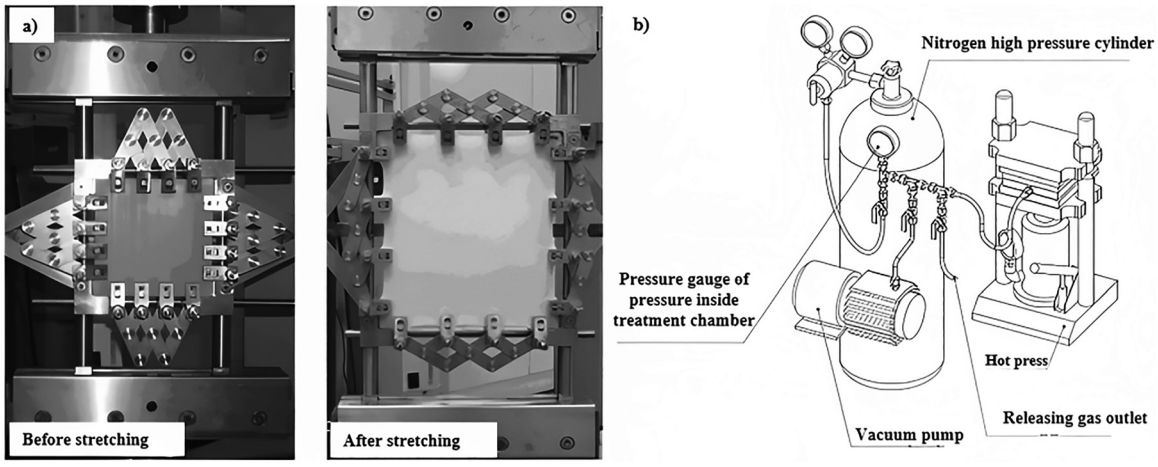

Figure 9: The experimental setups developed (a) bi-axial stretching machine and (b) schematic diagram of the expansion by gas treatment Qaiss and Bousmina (2011), Qaiss et al (2012).

sector, biomedical and aerospace industries (Chen et al. 2019; Duda and Raghavan 2016; Wang et al. 2017). For polymers, several studies were conducted based on the cited advantages and aimed to explore the potential of 3D printing in creating porosities and to study the influence of pore size and shape on the piezoelectric effect of printed piezocellular materials.

According to Assagra et al., the porous samples were developed by the GTMax3D 3D printer based on fused deposition modelling, where thermoplastic filaments are melted and extruded then deposited layer by layer according to a predefined pattern with a layer resolution of 0.05 to 0.3 mm (Assagra et al. 2016). The acrylonitrile butadiene styrene (ABS) was initially chosen over other several printing materials because of its improved electrical and mechanical properties (Palito et al. 2019). The elaboration procedure was performed by heat-sealing the edges of two 3D printed discs. The first being a dense disc of 38 mm diameter and 100 µm thickness and the second being a disc of 38 mm diameter with a total thickness of 200 µm containing open squares (one, four and sixteen squares) of 100 µm height that would constitute the porosity to be studied (see Figure 10).

However, Najihi et al. (2022) printed fully 3D porous samples without the need to use bonding techniques to join pre-printed structures separately. Here, a Markforged Marktwo printer was used to ensures that the resulting cavities will remain free of collapse, which can be seen in the transversal cut of the samples in (Figure 10c). Three configurations with elliptic cylinder pores were investigated in which the size of the printed pores was modified but the porosity percentage is fixed to 23.5 mm^3 in order to visualize the effect of changing pore size on the piezoelectric coefficient d_{33}. A new conception was proposed by Palitò (Palitó et al. 2019) in which the 3D printing process leaves air spaces between two extruded filaments, stacked in opposite directions, forming a grid pattern.

3.6 Foaming agents

Foaming agents are materials that, in the vapor phase, causes the expansion of a molten polymer during pressure reduction (Lee and Park 2014), they can be either physicals or chemicals. The difference is that physical foaming agents (PFAs) provide gas for the expansion of polymers by

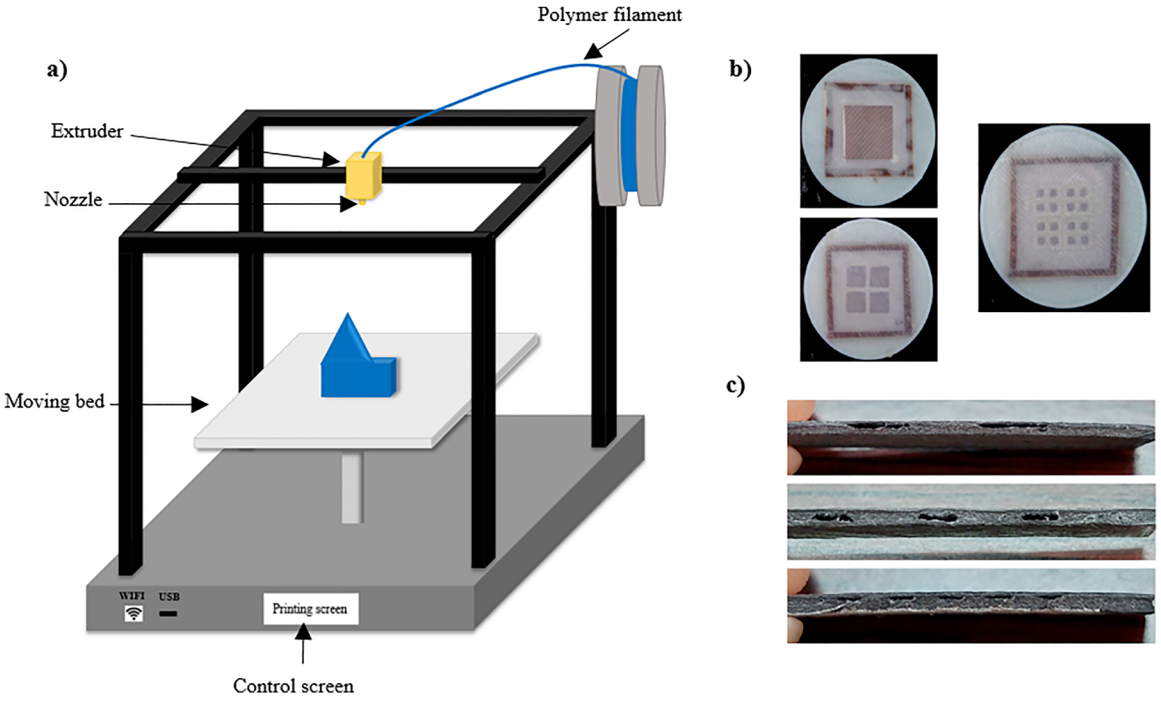

Figure 10: Fused deposition modelling technique, (a) 3D printing machine, (b) cellular samples established by the 3D method with squar cavities (Assagra et al. 2016) and (c) elliptic cylinder (Najihi et al 2022).

changing the initial physical state either by the volatilization (boiling) of a liquid or by decompression of a compressed gas to atmospheric pressure after being incorporated into a molten polymer under pressure like the supercritical fluids discussed in the previous section. While chemical foaming agents (CFAs) generate gases as chemical reaction products that results of the decomposition of the original molecule, producing gases for polymer expansion and solid residues that remain in the foamed polymer. For the extrusion foaming process of unfilled thermoplastics, CFAs come in two categories, endothermic and exothermic. The endothermic property was considered beneficial since the foaming agent releases a gas (such as CO_2 and N_2) when subjected to heat which leads to bubble nucleation and the constitution of a porous structure. In addition, the CFA absorbs heat during its decomposition, which provides cooling for the polymer, increases the viscosity, stabilizes the cell structure and prevents cell interfusion (Heck 1998).

In this framework, Porous thin films were designed by Ennawaoui et al. (Ennawaoui et al. 2019) in a semi-pilot extrusion line consisting of three single-screw extruders feeding a die to coextrude three layers. A film of porous ethylene vinyl acetate EVA was made by dry blending the chemical foaming agent hydrocerol at different concentrations (0.1 and 2 %) with the EVA and then flow through the main single-screw extruder operating at 30 rpm with a specific temperature profile from the hopper to the extruder exit. Then, two thin layers of pure EVA were made by the other two peripheral single-screw extruders operating at 30 rpm and at constant temperature along the extruder. Later, a tri-layered EVA-porous EVA-EVA sandwich was co-extruded to ensure closed-cell morphologies and regularity of the porous EVA surfaces, for best electrode deposition and polarization (see Figure 11). The coextrusion technique demonstrated positive morphological outcomes compared to hot pressing of the EVA-porous EVA-EVA sandwich (Derraz et al. 2022).

4 Electrode deposition or film metallization

After the creation of the cellular structure of the polymeric film, the deposition of electrodes or the metallization is an essential step to proceed to the ionization and the activation of the piezoelectric-like effect (Ramadan, Sameoto, and Evoy 2014), the electrodes are essential to accumulate electrical charges and to collect the response and carrying it to the measuring systems. Metallization consists on coating the surfaces of the polymer film with a conductive material such as copper, nickel or aluminum in order to connect the charges on each surface of the film and thus be able to

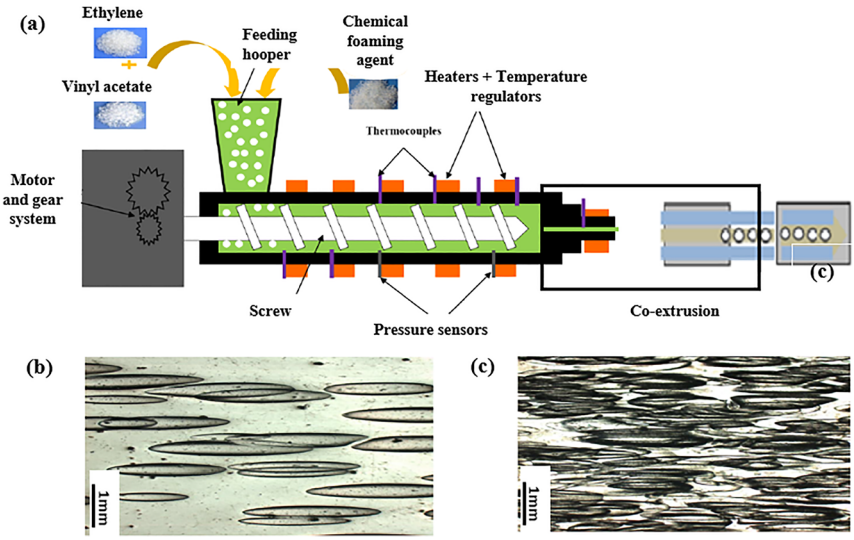

Figure 11: Extrusion process for the production of piezoelectric-like porous EVA thin films, with an Optical microscopy image of the porous polymer with different percentage of foaming agent (Ennawaoui et al. 2019).

control the potential difference between the two surfaces (Bobinger et al. 2019).

For the production of so-called thin films with a thickness ranging from a few nanometers to a few of micrometers, vapor deposition is the most widely used dry coating method for polymers. There are two main categories of vapor deposition: CVD chemical vapor deposition and PVD physical vapor deposition. Both technologies involve three essential elements. First, a source of material to be deposited called target (metallic or ceramic as well as precursors containing the elements to be deposited); second, a piece to be coated on which the deposit from the source will condense; and finally, a medium in which the mass transfer occurs (place of the physical or chemical phenomenon in question) (Martín-Palma and Lakhtakia 2013). In the case of CVD, the source material is not pure, but it is mixed with a volatile precursor used as a support that react and/or decompose on the surface of the substrate to produce the desired deposit. The mixture is injected into the chamber containing the substrate and then deposited there. Once the mixture is adhered to the substrate, the precursor eventually decomposes, leaving the desired layer of source material in the substrate. The decomposition process can be assisted or accelerated through the use of heat, plasma or other processes (Choy 2003). However, in PVD, the material to be deposited is initially massive, with a specific geometry (cylindrical, wired) and a variety of possible materials (metals, alloys, and ceramics). This material is exposed to a plasma (typically Ar) of ions and electrons that are used to "knock" off the target material and make a cloud of source atoms (in the case of sputtering (Swann 1988)) (see Figure 12) or evaporated by heating to high temperatures where they melt and then evaporate or sublimate into a vapor within the vacuum chamber. In this way, atoms are torn from the target and deposited on the surface of the part to be coated. This type of coating can be likened to a condensation phenomenon on the surface of the part to be coated.

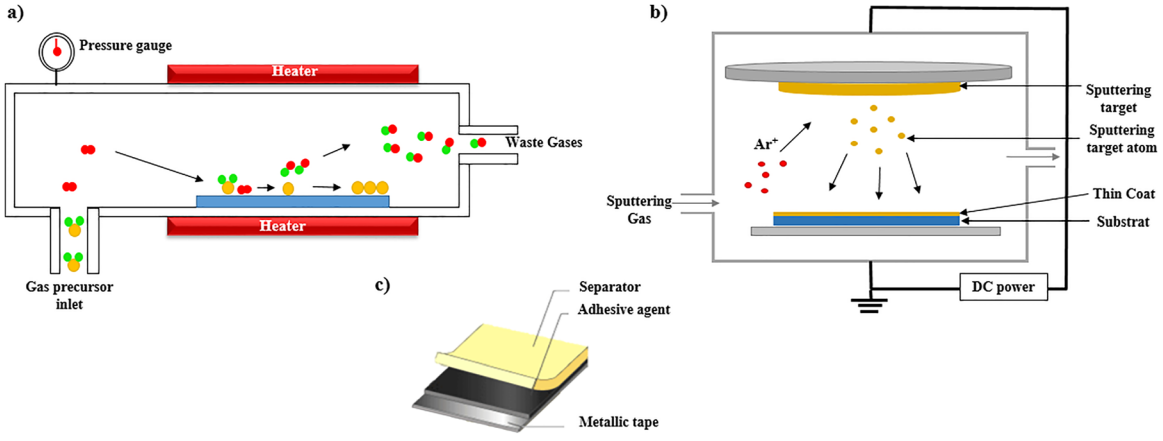

Figure 12: Metallization techniques; (a) Chemical and (b) physical vapor deposition, and (c) conductive tape.

An easy way for depositing conductive layers on insulating substrate is using a conductive strip that consists of a conductive adhesion agent attached to a metal tape and a separating film that would be removed so that the metallic coating sticks to the polymer surface (Lai et al. 2021) (Figure 12c). Polymer films can also be electrode with conductive epoxy (Hall et al. 2005). However, conductive epoxy electrodes showed significant reduction of the dielectric and piezoelectric measured constants (Sherrit et al. 1991).

One of the major difficulties in achieving a highly adhesive metallization is the structural incompatibility between the polymer and the metal. Conventional processes to promote adhesion between an electrodeposited metal layer and a polymer substrate resides in making morphological changes in the polymer surface such roughening or smoothing, which can be treated by the mean of plasma treatment, mechanical processes or wet chemical processes, such as the use of organic blowing agents (Martin 2010).

5 Charging methods or ionization

Ferroelectric materials do not exhibit a sufficient piezoelectric effect due to their large number of small crystals with random orientations of their microscopic domains, unless they are submitted to a high electric field that will aligns the crystal orientations (Dineva et al. 2014). However, for cellular polymers, the piezoelectricity is an artificial property that required the ionization of gas molecules inside the pores using an electric field to provide electrical charges and align them in order to establish a dipolar moment. Charges of opposite polarity are subsequently enclosed on the top and bottom surfaces of the voids, depending on the applied electric field direction (Qiu 2010). Ionization is the action of removing or adding charges to an atom or molecule. The atom or molecule losing or winning charges is no longer electrically neutral, it is then called an ion.

The ionization of gases can generally be performed by radiation with a sufficient wavelength to eject this peripheral electron. When the ionizing radiation consists of photons, this is called photo-ionization (Lifshitz and MärkLindon 1999) (this is the case in planetary nebulae). In addition, if a gas receives enough thermal energy, its average energy becomes equal to or greater than its ionization energy. The constituents of this gas can, therefore, be ionized because of the shocks between the atom/molecule (Wieser and BrandLindon 1999), this is what happens in the solar corona (Dzifčáková and DudíkLivadiotis 2017). Ionization can also occur when a molecule reacts with a reactive ion which results in electron transfer or the creation of adducts (Koenig and Koenig 1999). However, the commonly used ionization methods in literature are the electrical contact poling and the Corona discharge.

The Contact poling, shown in Figure 13, is a classical polarization method requiring direct contact of the live electrode with the sample electrode and the application of a very large electric field (DC voltage) to enable the sample to be polarised. The samples must be covered with both top and bottom electrodes (Gerhard-Multhaupt et al. 2002). However, the application of large DC fields or imperfection during the metallization process results in dielectric breakdown of the sample that may lead to a continuous electric arc damaging the material. These difficulties often result in materials polished at insufficient electric fields, below the permitted dielectric breakdown threshold, to overcome this; the samples must be placed in an electrically insulating fluid bath (Rupitsch 2019).

The most used technique for charging the cellular polymers is the Corona discharge, illustrated in Figure 14, where the cellular film is placed on a metal plate and a needle is suspended over the center of the plate. The metal plate and needle are connected to the positive and the negative electrodes of a voltage generator, respectively. A conductive control grid can be inserted between the sample and the corona needle to ensure that the charged ions are uniformly distributed and to control the potential at the film surface. The control grid is connected to a separate power supply, which is maintained at a lower potential than the corona tip. Unlike the electrode method, corona ionization requires the metallization of only one side of the polymer film. This surface must be in contact with the plate which is bonded to ground.

When a high VN voltage is applied to the electrodes, the air between the electrodes becomes ionized and causes a flow of ions directed towards the sample (Belhora et al. 2013). The ions create a layer of charge on the surface of the sample, generating a polarization field through the sample to the ground plate below (Das-Gupta and Doughty 1978; Mahadeva et al. 2013). The position of the grid and the applied voltage control the number of charges deposited on the polymer surface also heating the plate guarantees a better ionization control (Belhora et al. 2012).

There are other polarization or ionization methods that are less commonly reported, such as electron beam

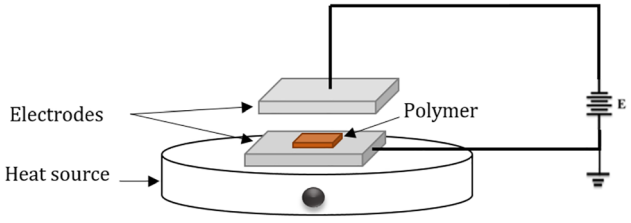

Figure 13: Electrode method.

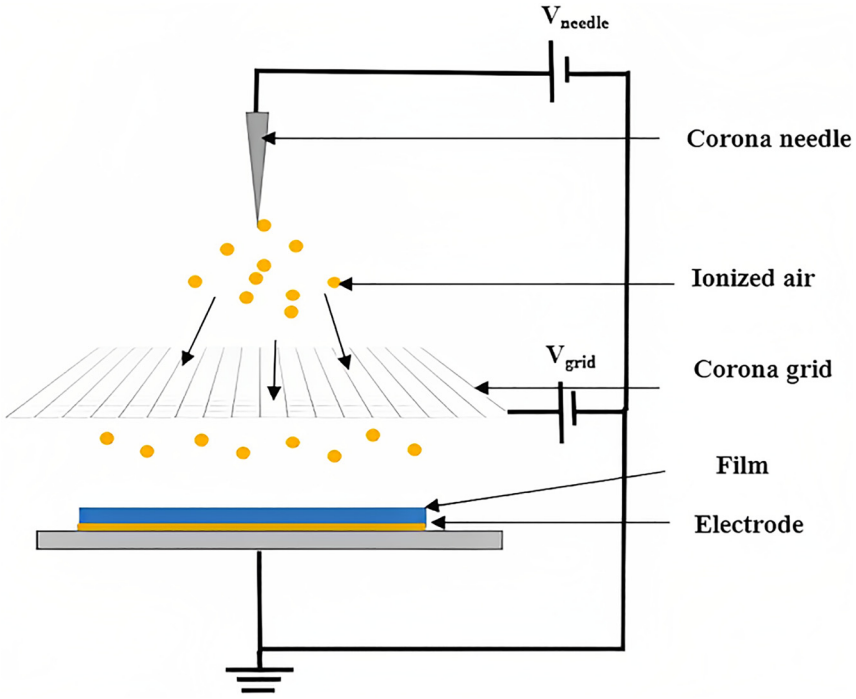

Figure 14: Corona discharge experimental setup.

polarization, where electron beam irradiation is used to deposit electrons on the surface of the piezoelectric polymer that causes the creation of dipoles, similar to the corona process. This method has the ability to locate certain areas of the film by a direct pattern with the focused electron beam, but it causes a chemical modification and degrades the material under the electric field (Šutka et al. 2018). Another interesting loading method is the use of flexible X-rays for ionization, which is mainly useful for piezo-cellular polymers (Hamdi, Mighri, and Rodrigue 2018).

Ionization methods show the importance of the existence of an ionizing gas inside the cells that give a shape to the film cells and promote the difference in potential between the cell surfaces by dropping positive and negative charges, and by the ionization power of the gas molecules. An explanation allowing the comprehension of the charging techniques is then presented in order to understand the dynamics of the electrical behavior in the air cavities of the material.

6 Breakdown

The process of gases ionization was explained by Townsend's theory in 1897, where free electrons are accelerated by an electric field and collide with gas molecules to emit more electrons. These electrons are in turn accelerated and emit more electrons (Townsend 1915). When an electric field is applied across a gaseous medium, the first ionization event creates a pair of ions; the positive one accelerates towards the cathode and the free accelerates towards the anode. If the electric field is strong enough, a free electron can gain enough energy to emit another electron the next time it collides with a molecule. The two free electrons then move towards the anode, drawing enough energy from the electric field and causing further impact ionization. As a result, the avalanche increases, free electrons are generated and electrical conduction through the gas is possible.

During the polarization process of cellular polymers, when the electric field applied to the air gap reaches an electric field threshold, the Townsend breakdown of the dielectric barrier discharge occurs and opposite charges are trapped in the upper and lower surfaces of the cells. The necessaryvoltage to start a discharge and induce piezoelectricity in cellular polymers is called the breakdown threshold potential V_{break}, it can be predicted by Paschen's law (Paschen 1889) as function of the product of the gas pressure and the distance between electrodes which is equal to the void height in the present context.

$$V_{\text{break}} = \frac{Apd}{\ln(Cpd) - \ln\left(\ln\left(1+\frac{1}{\gamma}\right)\right)} \tag{1}$$

where V_{break} is the breakdown potential (V), p is the pressure (Pa), d is the void height (m), γ is called the secondary electron emission coefficient, C is the saturation ionization in the gas, and A is related to the excitation and ionization energies. A and C are calculated experimentally while being specific to each gas. In the case of air, for example,

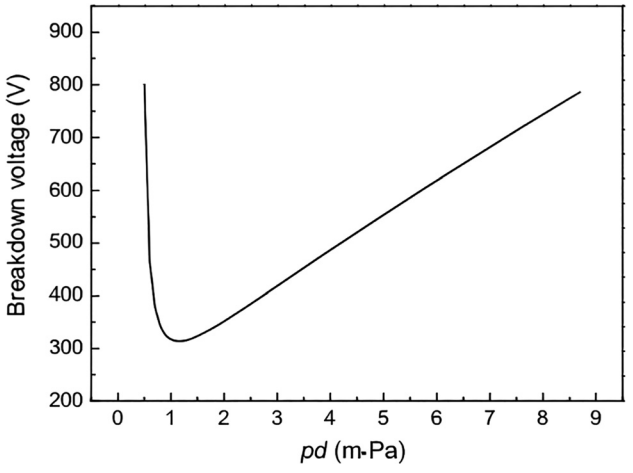

Figure 15: Paschen breakdown voltage as a function of the product pd for air gas.

$A = 273.8\ \mathrm{Vm^{-1}\,Pa^{-1}}$, $C = 11\ \mathrm{m^{-1}\,Pa^{-1}}$ and $\gamma = 0.01$. Figure 15 shows the influence of gap spacing between top and bottom electrodes on the air breakdown voltage. Always for air in the standard conditions of pressure and temperature, the necessary voltage to form an arc in a one meter void is about 3.4 MV. The electric field strength for this space is therefore 3.4 MV/m.

7 Piezoelectric behavior modeling

To facilitate practical applications, theoretical studies of piezoelectric cellular polymer films are necessary to optimize the output characteristics; this paragraph gives some developed models of properties such as permittivity, piezoelectric coefficient, to bring out the impacting parameters. Sessler was the first to develop a simplified model to determine the pseudo piezoelectric behavior of charged cellular polymers (Sessler and Hillenbrand 1999), where a representation of a thin film cut vertically looks like alternating layers of polymer and gas, as can be seen in Figure 16. This model served as a reference for later developed models.

The thicknesses of the polymer layers and the air layers are represented by d_{1i} and d_{2j} respectively, with $i = 1, 2, \ldots, N$ and $j = 1, 2, \ldots, M$, where N and M are the total numbers of each phase. The two solid surfaces confining the jth air layer carry a total planar charge of density σ_j and $-\sigma_j$, respectively, and the electric fields in the solid and air layers are noted E_{1n} and E_{2m}, respectively.

$$E_1 = -\left[\varepsilon_0\left(d_1 + \varepsilon_P d_2\right)\right]^{-1}\sum_j d_{2j}\sigma_j \tag{2}$$

$$E_{2i} = \sigma_i/\varepsilon_0 - \varepsilon_p\left[\varepsilon_0\left(d_1 + \varepsilon_P d_2\right)\right]^{-1}\sum_j d_{2j}\sigma_j \tag{3}$$

$$E_{1i} = E_1, d_1 = \sum_i d_{1i} \text{and}\ \ d_2 = \sum_j d_{2j} \tag{4}$$

The charge on the top electrode is given by $\sigma_0 = -\varepsilon_0\varepsilon_p E_1$. In the short circuit, it depends on the thickness changes of the film, caused by an applied force. When a pressure p is applied to the ferroelectret, change in thickness is observed because of compression in layers of air. Therefore, the electrode charge varies according to $\frac{\partial\sigma_0}{\partial d_2}$ therefore to E_1. From the stress–strain relationship $\frac{\Delta d_2}{d} = \frac{p}{Y}$, where, Y and is the film Young's modulus, $d = d_1 + d_2$ and p is the applied pressure. The piezoelectric coefficient is given by:

$$d_{33} = \frac{\Delta\sigma_0}{p} = \frac{\varepsilon_p d}{Y}\frac{d_1\sum_j d_{2j}\sigma_j}{d_2\left(d_1 + \varepsilon_p d_2\right)^2} \tag{5}$$

with the same interpretation of Sessler's model, Zhukov used the breakdown threshold of the electric field in the air gap E_B to express the remanent interface charge σ_{rem} (Zhukov et al. 2018), which is the interfacial charge σ_j after the applied voltage is turned off or the sample is short-circuited, in the d_{33} expression of a three layered film:

$$d_{33} = \frac{\varepsilon_0\varepsilon_p\varepsilon_g E_B}{Y}\frac{(2d_1 + d_2)}{\left(2\varepsilon_g d_1 + \varepsilon_p d_2\right)} \tag{6}$$

where ε_g and ε_p are, respectively, the gas and the polymer dielectric constants.

Considering charge diffusion according to Fick's law, Najihi et al. (2021) showed that the piezoelectric coefficient d_{33} can be written as a function of the effective diffusion coefficient of charge displacement D_c, the porosity $\varnothing$, the total film thickness h, the number of layers n, and the time t. The model takes into account the expression for the surface charge density σ_j in all the polymer-gas interfaces as well as the formula for the Young's modulus of the porous film Y expressed in terms of the porosity $\varnothing$ and the Young's modulus of the nonporous matrix Y_0.

$$d_{33} = \frac{(1-\varnothing)\mathcal{E}_p}{Y\left(1-\varnothing+\mathcal{E}_p\varnothing\right)^2}\left(<\sigma_j> + \varnothing\left(1-\varnothing+\mathcal{E}_P\right.\right.$$
$$\left.\left.\varnothing\frac{\partial <\sigma_j>}{\partial\varnothing}\right)\right) \tag{7}$$

where $<\sigma_i>$ is the average value of electrical charge displacement at all polymer–gas boundaries.

$$<\sigma_j> = \frac{1}{n-1}\sum_{j=1}^{M}\sigma_j$$
$$= \frac{\sigma_0}{n-1}\int_1^M .\mathrm{erfc}\left(\frac{h\left(\frac{j(1-\varnothing)}{N} + \frac{(i-1)\varnothing}{M}\right)}{2\sqrt{t.D_c}}\right)d_j \tag{8}$$

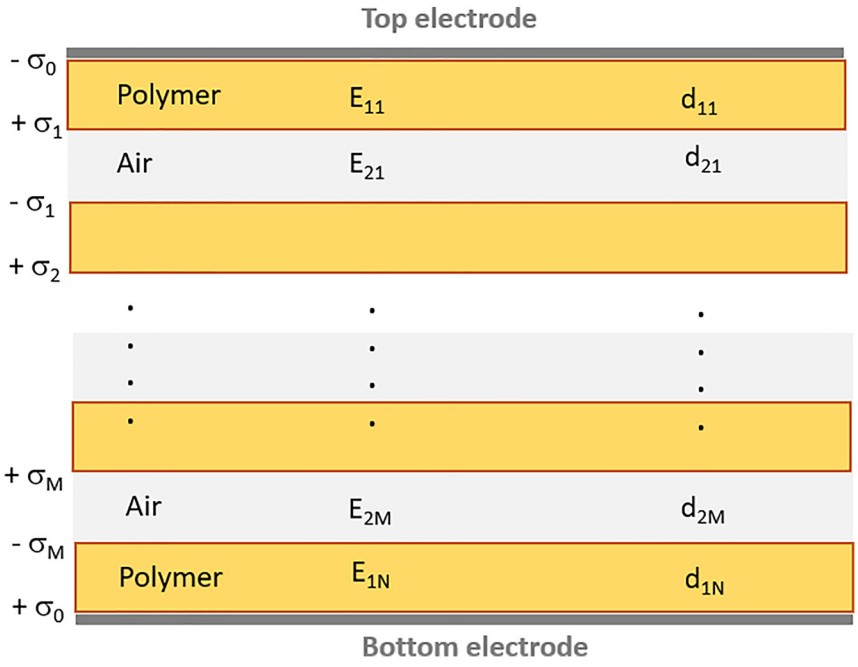

Figure 16: Simplified model of a cellular film develloped by Sessler.

Kacprzyk (Kacprzyk 2017) has presented another model for the piezoelectric response of two layers (a hard a and a soft layer b) with an interface charge σ at the double-layer boundary, permittivities $\varepsilon_{a,b}$, Young's modulus $Y_{a,b}$ and thicknesses $d_{a,b}$.

$$d_{33} = \sigma\left(\frac{1}{Y_a} - \frac{1}{Y_b}\right)\frac{\mathcal{E}_a\mathcal{E}_b d_a d_b}{\mathcal{E}_a d_b + \mathcal{E}_2 d_a} \tag{9}$$

A physical model of cellular piezoelectret generators was established by Li et al. (2016) to derive the output voltage V as it depends on the electret material properties (permittivity), device structure (surface S), polarization process ($Q_0 = \sigma_0 \times S$), and external load R.

$$\begin{aligned} V(t) = {} & Q_0\left(\frac{\varepsilon_g d_p}{\varepsilon_p d_{\text{air}-0}} + 1\right)\frac{d_p}{S\,\varepsilon_0\varepsilon_g} \\ & - Q_0\frac{\varepsilon_g d_p}{S\,\varepsilon_0\varepsilon_g d_{\text{air}-0}}\left[\frac{d_p}{\varepsilon_p} + \frac{d_{\text{air}}(t)}{\varepsilon_g}\right]e^{\frac{-1}{RS\varepsilon_0}\left[\frac{d_p}{\varepsilon_p}t + \int_0^t \frac{d_{\text{air}}(m)}{\varepsilon_g}\,dm\right]} \\ & - Q_0\left(\frac{\varepsilon_g d_p}{\varepsilon_p d_{\text{air}-0}} + 1\right) \times \frac{d_p}{RS^2\varepsilon_0^2\varepsilon_P} \times \left[\frac{d_p}{\varepsilon_p} + \frac{d_{\text{air}}(t)}{\varepsilon_g}\right] \\ & \times e^{\frac{-1}{RS\varepsilon_0}\left[\frac{d_p}{\varepsilon_p}t + \int_0^t \frac{d_{air}(m)}{\varepsilon_g}\,dm\right]} \times \int_0^t e^{\frac{1}{RS\varepsilon_0}\left[\frac{d_p}{\varepsilon_p}m + \int_0^t \frac{d_{\text{air}}(x)}{\varepsilon_g}\,dx\right]}dm \end{aligned} \tag{10}$$

Ennawaoui et al. suggested a model that allows the determination of the power density based on cell porosity, thickness, and dielectric constant of porous polymers, to get (Ennawaoui et al. 2016):

$$P = 2\pi^2 R_1 \frac{\left(\sigma\left[\frac{\frac{\varepsilon_g}{\varepsilon_p}\left(1+\frac{d_g}{d_p}\right)}{\left(\frac{\varepsilon_g}{\varepsilon_p}+\frac{d_g}{d_p}\right)^2} f A S_m\right]\right)^2}{1 + 4\pi^2\left(\varepsilon_{33} - \sigma^2\left[\frac{\frac{\varepsilon_g}{\varepsilon_p}\left(1+\frac{d_g}{d_p}\right)}{\left(\frac{\varepsilon_g}{\varepsilon_p}+\frac{d_g}{d_p}\right)^2}\right]^2\right)^2\left(\frac{R_1 f A}{e}\right)^2} \tag{11}$$

where R_1 is the resistor through which power is dissipated. A is the surface of the polymer (covered with electrodes), σ is the charge density, S is the strain and f is the resonance frequency.

Hillenbrand, Pondrom, and Sessler (2015) recommended a model for the power generated, as a response to an excitation, by a cellular polymer:

$$P = \frac{m_s^2 R_l d_{33}^2 \omega^2 a^2}{\left[\left(\frac{\omega^2}{\omega_0^2} - 1\right)^2 + 4\xi^2\frac{\omega^2}{\omega_0^2}\right]\left[1 + (R_l C_s \omega)^2\right]} \tag{12}$$

where m_s is the seismic mass, R_l is the load resistance, C_s is the capacitance, ω_0 is the resonance frequency, ω is the circular frequency and ξ is the damping ratio.

For the inverse piezoelectric effect, Paajanen modeled the sensitivity of the thickness actuator (Paajanen, Valimaki, and Lekkala 1999), i.e., When an external voltage V is applied to the electrodes and increased from 0 to V, the film thickness changes by an amount Δx.

$$\Delta x = \frac{x_0 \frac{1}{2} \varepsilon_0 \varepsilon_p^2 V^2 - \varepsilon_P d_p \sigma_{\text{eff}} V}{Y \left(d_p + \varepsilon_p d_g\right)^2} \quad (13)$$

where σ_{eff} is the effective charge density on the polymer/air interfaces on both sides of each air gap and x_0 is the thickness of the unstressed film.

8 Electromechanical performance of piezoelectric cellular polymers

The application of mechanical or electrical excitations lead the charged voids to act as macroscopic diploes and showing piezoelectric-like behaviors. Relative to conventional piezoelectric polymer materials (ex: PVDF), piezoelectric foams of different manufacturing methods have shown promising piezoelectric responses which makes this material a candidate for energy harvesting (see Table 1).

In order to investigate the electromechanical performance of ferroelectric materials, in particular the piezoelectric coefficient (d_{33}) which is the amount of electrical charge induced Q when a unit of force is applied F_a ($d_{33} = Q/F_a$), Two measuring techniques are commonly used for determining the piezoelectric coefficient; the quasi-static and dynamic method. The quasi-static that consist on applying an external force of $F_a = mg$ (where g is the acceleration of the gravity) to the sample by manually adding and removing a mass m out of the surface of the sample in the z direction, then the induced charge Q is simultaneously measured with an electrometer (Hillenbrand and Sessler 2004). Several generators for energy harvesting work under quasi-static excitations where the d_{33} value is averaged over several exercises of setting up and removing the mass (Jiao et al. 2021; Wang et al. 2021a).

The dynamic measurement of d_{33} is obtained by accelerating sinusoidally the sample and a mass on it by a shaker, therefore the sample is subjected to static $F_a = mg$ and dynamic $F_d = ma$ force (where a is the acceleration). The d_{33} can be measured over a frequency range by making the shaker input signal vary in frequency for different sample masses and surfaces.

Dielectric spectroscopy is also an important technique to characterize the electrical performance of the porous polymers. It permits to assess the dielectric identity of a polymer by determining the permittivity (ε_r) which is the ability to polarize a material subjected to an electric field and the capability to store a charge or to serve as a capacitor, and the electrical loss as an indicator of the energy dissipation of the dielectric material (tan δ). These two parameters are related and can be calculated from measurements of to the capacitance (C) (Licari et al. 2011).

In order to enhance the piezoelectric performance of piezoelectric cellular polymers, studies were done about the impact of porosity percentage on the piezoelectric coefficient and it was shown that it increase with the increase of porosity implicitly is by the number or the thickness of pores (Ennawaoui et al. 2019; Ennawaoui et al. 2021; Kierzewski et al. 2020; Qaiss et al. 2013). In addition, forming a multilayer structure through stacking ferroelectrets in layers lead to increase the output, by finding the best-performing stacking sequence which optimizes the macro-dipole numbers and the elastic moduli for the entire film stack (Wang et al. 2021b).

9 Applications

The piezoelectric energy harvesters replace the need for networked energy, as they are effective in powering small devices in situations where the accessibility or the environmental conditions limit the integration of electrical cables or batteries. Sensors/generators based on piezoelectric porous polymers are proposed, designed and marketed to empower smart systems, medical devices, automobiles, and sound generators.

Based on cellular polymers, sensors have been developed recently for biomedical applications due to their lead-free composition. They were used to detect the activities of the human body by acquiring the muscles activity, and recording it to provide a diagnosis that contributes to healing (Dobkin and Dorsch 2011). In the case of limb amputation, which is a major hurdle for amputees and limits their performance in daily exercises, and since prostheses are the solution, piezoelectric sensors have been combined with surface electromyography (sEMG) for the rehabilitation to provide quantifiable information on the myoelectric output of a muscle. According to Jarrasse (Jarrasse et al. 2017), the activity of residual limbs was recorded while participants performed phantom hand movements, and then they synchronously mimicked the movement of the phantom limb with their intact hand (Figure 17). Due to the bending of the piezoelectric sensor in touch with the intact hand kinematics were recorded, and then the sEMG data of the residual limb were classified with the corresponding movement of the phantom limb.

Another sensor based on voided Polypropylene piezoelectric film with d_{33} value of 510 pC/N was used to obtain the pulse signals over the radial artery at the wrist (Nie et al. 2019). As shown in Figure 18, the sensor consists of a piezoelectret film covered with metallic electrodes, a wooden cylindrical piece that provide the external pressure between the sensor and the skin, and a medical clip used to fix the

Table 1: Elaboration characteristics and responses of some cellular piezoelectric polymers.

Polymer matrix	Porosity creation technique	Thickness (um)	Poling technique	Poling voltage (KV)	d_{33} (pC/N)
Polypropylene (PP) Sessler and Hillenbrand (1999)	–	70	Corona discharge	–	200
Fluoro-ethylene-propylene (Teflon FEP) Altafim et al. (2006)	Hot pressing + vacuum aspiration	125	Impulse voltage in a small air gap	–	550
Isotactic polypropylene (IPP) Hillenbrand et al. (2006)	Biaxial stretching of IPP containing particles	50	Corona discharge	Needle: 20 Grid: 0.5	–
Polytetrafluoroethylene (PTFE) and fluoroethylenepropylene (FEP) Zhang et al. (2006)	Hot pressing by template	50	Corona discharge	Needle: 32	>1000
Polyethylene-naphthalate (PEN) Fang et al. (2007)	Foaming in supercritical carbon dioxide, inflation, biaxial stretching	100	Corona discharge	Air at atmospheric pressure: 21 Sulfur hexafluoride (SF6) at a pressure of 3 bars: −50	140
Poly(ethylene Terephthalate) (PET) Wirges et al. (2007)	Treatment in supercritical CO_2+ biaxial stretching+ Inflation	–	Corona discharge	Between −20 and −60	470
Fluoroethylenepropylene (PEN) Altafim et al. (2009)	Tubular template based	–	Direct contact	–	>160
Acrylonitrile butadiene styrene (ABS) Assagra et al. (2016)	Three-dimensional (3D) printing	300	Direct contact	4.5	100
Polypropylene (PP) Jarrasse et al. (2017) Effect of processing conditions on the cellular morphology of polypropylene foamed films for piezoelectric applications.	Supercritical nitrogen + Blowing agent	–	–	–	–
Polypropylene Qaisset al. (2012)	Biaxial stretching of pp containing macroparticules + gas inflation	85	Corona discharge	20	450
Polypropylene (PP) Nie et al. (2019) Understanding the role of the gas in the voids during corona charging of cellular electret films-a way to enhance their piezoelectricity.	Biaxial stretching of PP containing impurities	70	Corona discharge in N_2 at 450 kPa	60	270
Poly(ethylene-co-vinyl acetate) Ennawaoui et al. (2021)	Chemical foaming agent + coextrusion	320	Corona discharge in silicone oil	–	5.1
Fluorinated ethylene propylene (FEP) Zhukov et al. (2018)	Hot pression of cylindrical tubes	350	Direct contact charging	6	160

sensor and generate three force levels during the pulse recording process. The system was used to evaluate the human body health by comparing the output with known health conditions through the analysis of the value of the approximate entropy (ApEn).

Relative to human body energy harvesting and health monitoring, zhou et al. investigated, as shown in Figure 19, a cellular polypropylene based generator for detecting coughing action and pulses (Wu et al. 2015). The sensor was fabricated via pressure expansion and reached a maximum peak power density of $\approx 52.8\,\mathrm{mW\,m^{-2}}$, Its d_{33} coefficient was stable at around 200 pC/N for six weeks measured under a temperature between 30 °C and 60 °C. For the same purpose, Fang et al. (2021) proposed a wearable piezoresistor-piezoelectret sensing system with "quasi applanation tonometry" method for pulse detection, where an adjustable static pressure was applied on wrist to compress artery and pulse signals were simultaneously recorded at the same position.

For acoustic implementations, piezoelectrics were used to reproduce the biosonar system of bats, which emit high-frequency sound signals and listen (receive) the echoes to locate prey and move in the dark. For this purpose,

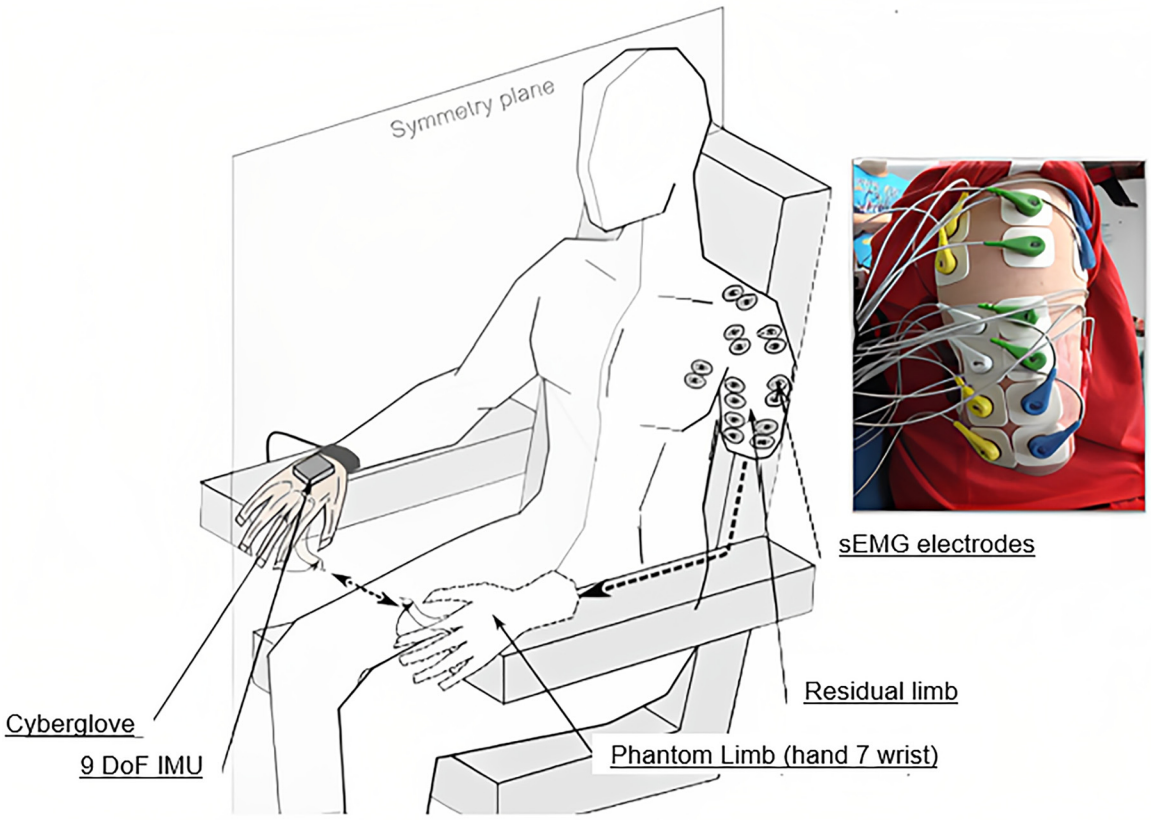

Figure 17: Sensor placements on participant's residual limb (Jarrasse et al. 2017).

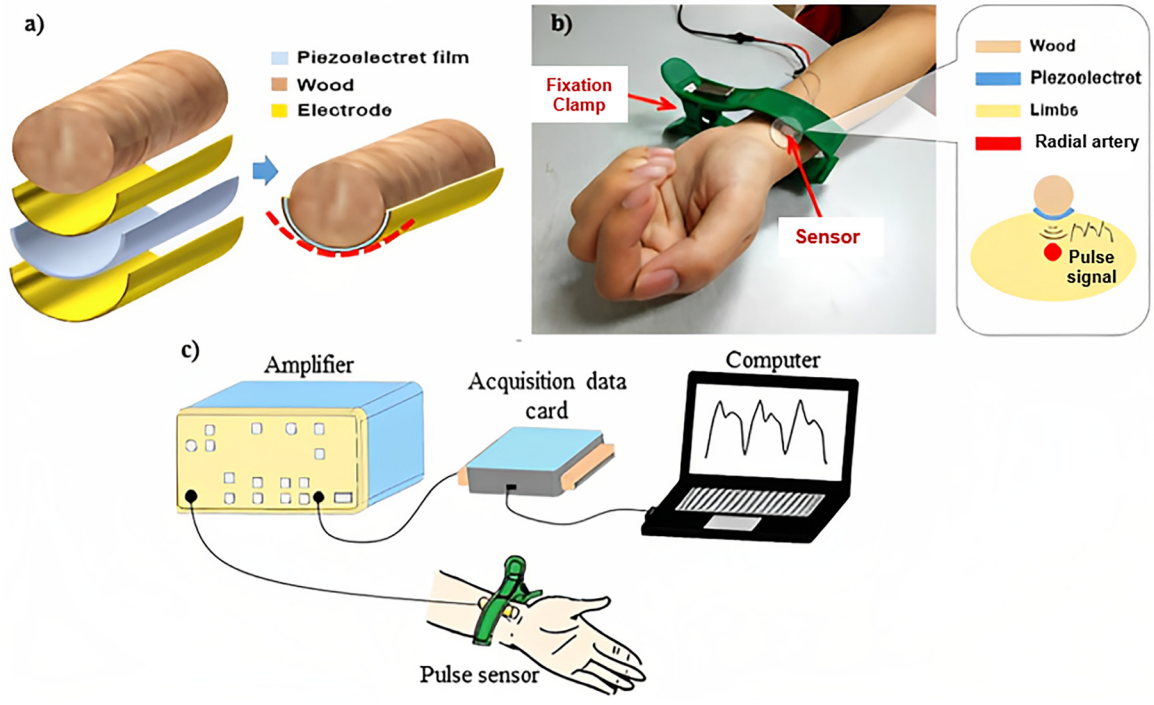

Figure 18: The pulse sensor, (a) the structure, (b) the artery pulse sensing system, and (c) schematic diagram for the experiment setup (Nie et al. 2019).

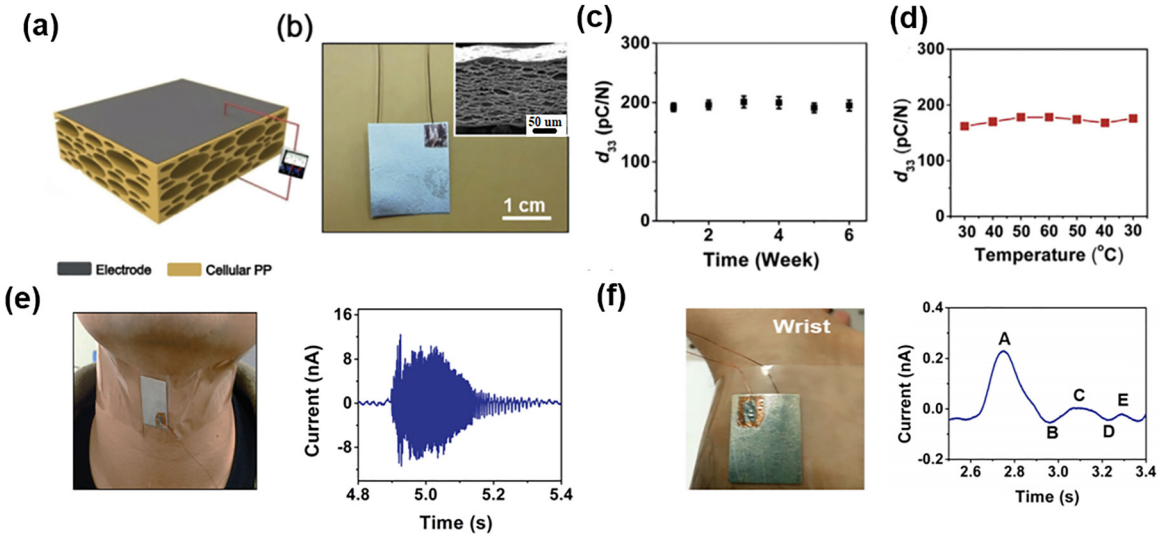

Figure 19: Health monitoring sensor, (a) a schematic illustration of a cellular polypropylene based sensor, (b) a photograph of the device and a SEM of the porosity, (c) the variation of the piezoelectric coefficient of the sensor for weeks and (d) under varying temperatures, (e) a photograph of the sensor on the throat and the enlarged view of the current signal generated by one coughing action and (f) a photograph of the wrist sensor and the view of the current signal generated by the arterial pulse (Wu et al. 2015).

artificial acoustic components, one emitter and two receivers, for a bat head were constructed using ultrasonic transducers made of piezoelectric cellular polymers, as well as the exploration of these materials as cavitation sensors to increase the efficiency of the ultrasound cleaning process (Rupitsch et al. 2011). Still in the field of sound, ferroelectret sensors are used for optimizing the comfort and reducing the noise in vehicles. Noise generating vibration is detected to determine the frequency and amplitude of the vibration. After recording, a sound wave of optimal frequency and amplitude (anti-sound) is generated and focused to cancel the noise in the human ears (Nykänen et al. 1999). Even in oceans, hydrophones piezoelectrets based are employed as an ultrasonic transducer for underwater detection (Palito et al. 2019).

For energy harvesting, a fluorinated polyethylene propylene (FEP) sensor was developed with a specific concentric tunnel structure using a template-based thermoplastic mold (Zuo et al. 2020) (see Figure 20). The functionality of two performance modes was investigated. The 33-mode energy sensor generated an output power of up to 1 mW at 210 Hz using a seismic mass of 33.4 g and an acceleration of 1 g. As for the 31-mode energy sensor, the output power of 15 μW was obtained at a relatively small resonant frequency of 26 Hz and a very light seismic mass of 1.9 g.

A paper-based active tactile sensor array (PATSA) composed of a PP piezoelectret was fabricated to act like calculator (Zhong et al. 2015). The mechanical pressure applied on the calculator are converted it into an electrical signal that is recorded and analysed to address the position and pressure information (Figure 21). Klimiec et al. (Klimiec et al. 2020b) evaluated the activity of human footsteps as an energy source. They have developed a ferroelectric film that they have placed in a shoe sole. When the foot presses on the piezoelectric film at each step, a voltage appears and allows a capacitor with a capacitance of C = 0.1 f to be charged at each pressure.

Another research developed a sensor capable of detecting surface textures (Sotgiu et al. 2022). As illustrated in Figure 22, the sensor is based on a ferroelectret material made from a cellular fluorinated ethylene propylene (FEP) film with hemispherical poly(dimethylsiloxane) (PDMS) bumps on the surface. The sensor was charged by a pyroelectric method newly developed by the same team (González-Losada et al. 2022). The interest of the sensor lies in its ability to mimic the response of mechanoreceptors present in human skin. When a finger explores a surface, the interaction between the skin and the roughness of the surface causes mechanical vibration waves to propagate through the skin of the finger and induce the mechanoreceptor response. The ferroelectret

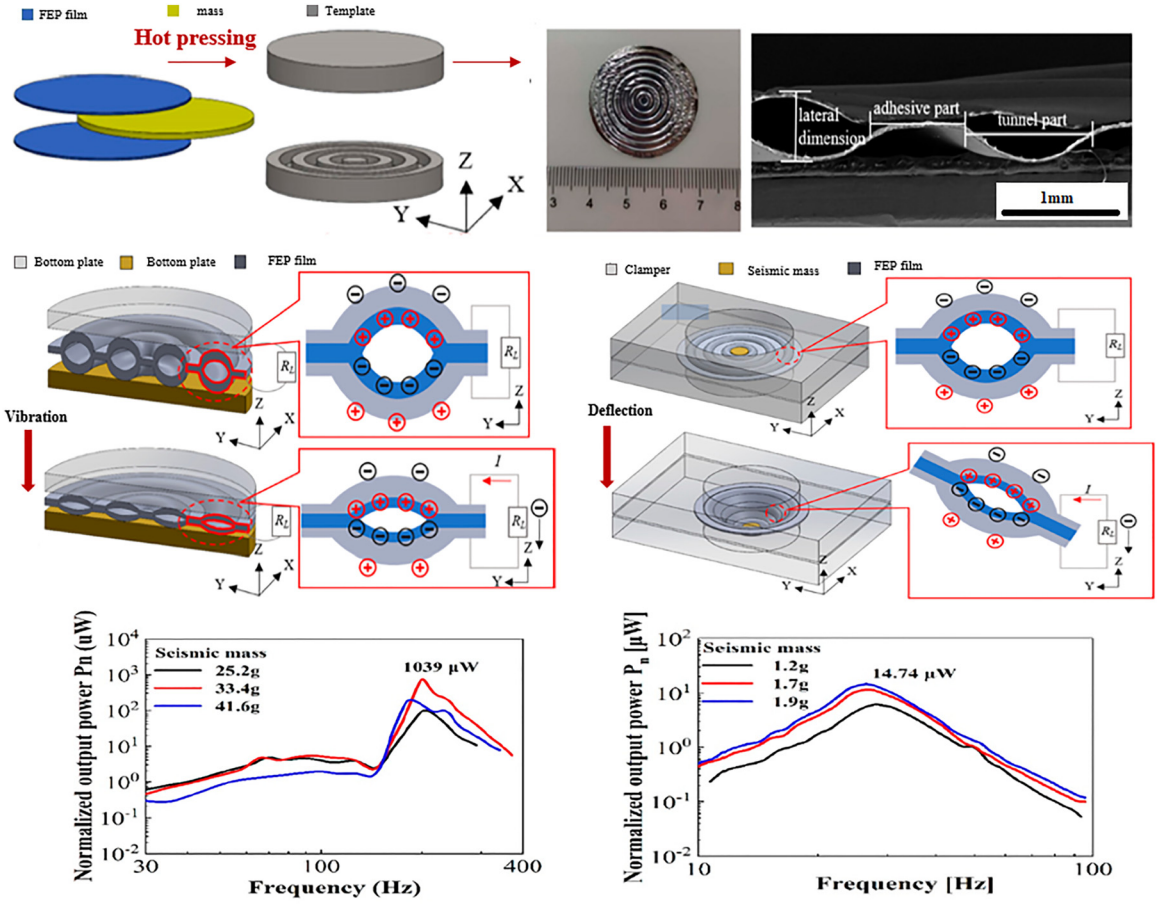

Figure 20: Schematic of fabrication, (a) optical image, and (b) cross-sectional SEM image of concentric tunnelfluorinated polyethylene propylene (FEP) film. (c–d) Schematic model and working mechanism of the 33-mode and 31-mode energy harvester, respectively. (e–f) The normalized output power of of the 33-mode and 31-mode energy harvester, respectively (Zuo et al. 2020).

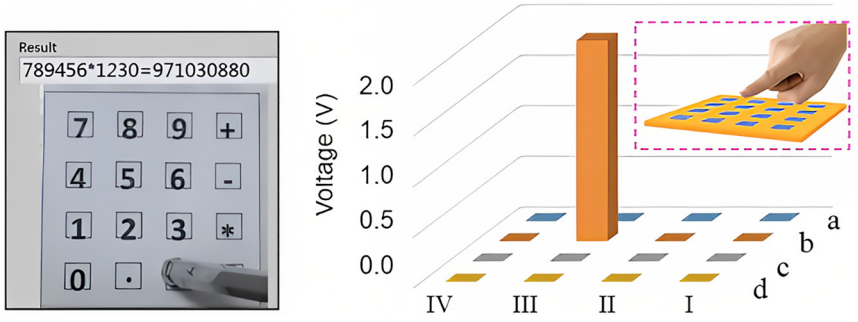

Figure 21: Prototype of a piezoelectric calculator and the voltage data plot harvested from a channel electrodes of the PATSA when pixel (III-b) was subjected to a force (Klimiec et al 2020b).

sensor is able to encode the mechanical vibration signals caused by the contact between the skin and the surface, thus allowing the perception of surface textures. The sensor had showed a piezoelectric coefficient of 150.1 ± 3.2 pC/N in response to an applied force in the range of 0.5 to 2 N.

Cellular polymers proved an excellent performance for energy recovery after the piezoelectric effect is caught. They were able to recover high powers that rivaled piezoelectric ceramics. A long way was crossed to meet the above mentioned achievements and another one to come for the improvement of the harvested response and the charge stability.

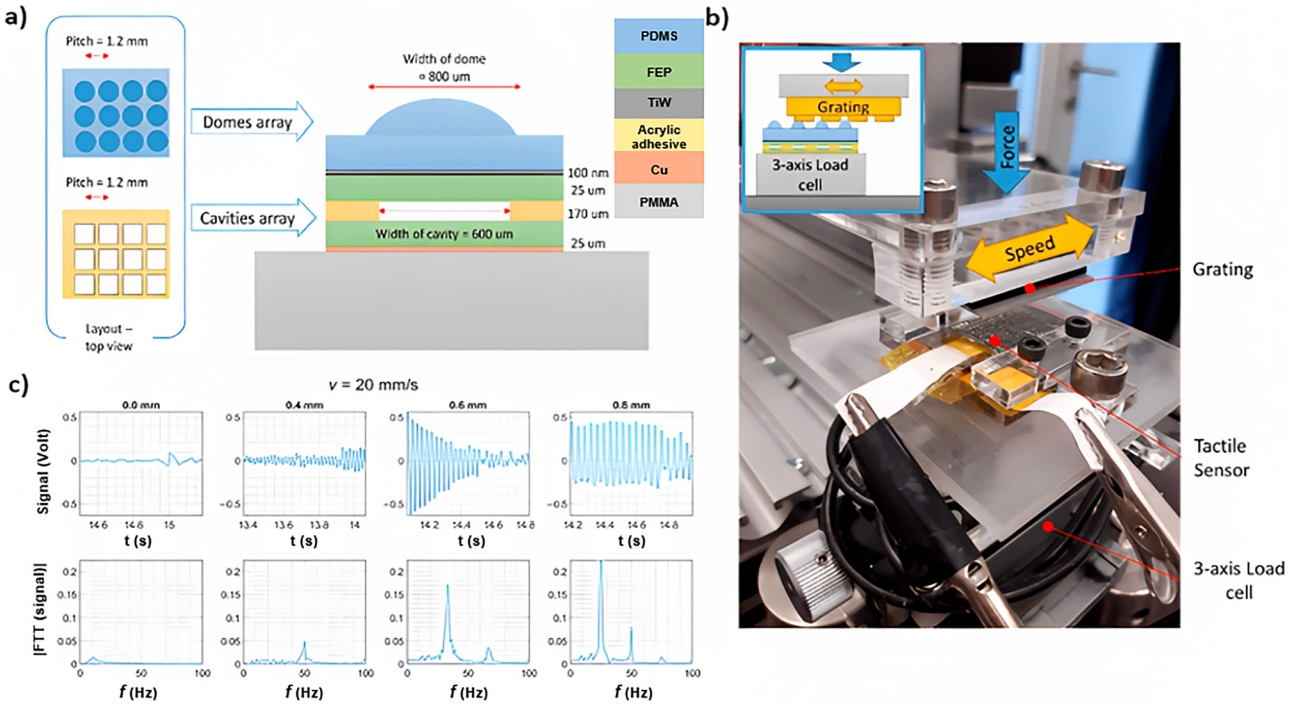

Figure 22: Surface textures sensor, (a) Illustration of the sensor using FEP and PDMS with an array of bumps on top, (b) experimental setup of the tactile sensor fixed on top of the load cell and (c) the signal when the sensor is scanned over the smooth and patterned surfaces with different spatial wavelengths (0, 0.4, 0.6, 0.8 mm) at scanning speeds of 20 mm/s scanning speed (Sotgiu et al. 2022).

10 Conclusions

This article provides an interesting bibliographical review on the elaboration techniques of cellular films as well as the necessary steps to undergo for obtaining the piezoelectric effect. Additionally, it highlights the diverse applications of porous piezoelectric polymers in various fields. The creation of porosity is a fundamental step in the development of these films, and several methods, including molding, printing, and thermal forming, allow for precise control of porosity, compared to the use of foaming agents as a microfabrication method. Since a high electric field is required, Electrical charging as well remains a crucial step for placing charges into the voids of cellular polymers in order to gain the piezoelectric-like activities and an efficient piezoelectric response. Charged porous polymers or piezoelectrets are distinguished from other piezoelectric materials by their flexibility, good impact resistance, lightweight and their ability to be created and optimized to improve their response. Owing to their artificial dipoles, piezoelectric polymer-foam are a promoting issue for energy harvesting. Charged porous polymers or piezoelectrets are distinguishable from other piezoelectric materials due to their flexibility, good impact resistance, lightweight, and their potential for optimization to improve their response. The creation of artificial dipoles in piezoelectric polymer-foam is a promising development for energy harvesting. Ongoing research aims to improve the temporal and thermal stability of charged polymers under variable conditions while maintaining their properties. Overall, this article provides a thorough and informative overview of the techniques, benefits, and applications of porous piezoelectric polymers.

Author contributions: All the authors have accepted responsibility for the entire content of this submitted manuscript and approved submission.
Research funding: None declared.
Conflict of interest statement: The authors declare no conflicts of interest regarding this article.

References

Altafim, R. A. C., H. C. Basso, R. A. P. Altafim, L. Lima, C. V. de Aquino, and L. G. Neto. 2006. “Piezoelectrets from Thermo-Formed.” *Bubble Structures of Fluoropolymer-Electret Films* 13 (5): 7.

Altafim, R. A. P., X. Qiu, W. Wirges, R. Gerhard, R. A. C. Altafim, H. C. Basso, W. Jenninger, and J. Wagner. 2009. “Template-Based

Fluoroethylenepropylene Piezoelectrets with Tubular Channels for Transducer Applications." *Journal of Applied Physics* 106 (1): 014106.

Assagra, Y. A. O., R. A. C Altafim, J. P. P. do Carmo, and R. A. P. Altafim. 2016. "Well-Defined Piezoelectrets Fabricated with 3D Printing Technology." In *2016 IEEE International Conference on Dielectrics (ICD)*, 257–9. Montpellier: IEEE.

Audet, E., F. Mighri, D. Rodrigue, and A. Ajji. 2018. "Cellular Morphology Optimization of Polypropylene/$CaCO_3$ Composite Films Designed for Piezoelectric Applications." *Cellular Polymers* 37 (3): 103–19.

Belhora, F., P.-J. Cottinet, D. Guyomar, L. Lebrun, A. Hajjaji, M. Mazroui, and Y. Boughaleb. 2012. "Hybridization of Electrostrictive Polymers and Electrets for Mechanical Energy Harvesting." *Sens. Actuators Phys.* 183: 50–6.

Belhora, F., P.-J. Cottinet, D. Guyomar, L. Petit, L. Lebrun, A. Hajjaji, M. Mazroui, and Y. Boughaleb. 2013. "Optimization of Energy Harvesting Conversion Using the Hybridization of Electrostrictive Polymers and Electrets." *Sens. Actuators Phys.* 189: 390–8.

Bobinger, M., S. Keddis, S. Hinterleuthner, M. Becherer, F. Kluge, N. Schwesinger, J. F. Salmerón, P. Lugli, and A. Rivadeneyra. 2019. "Light and Pressure Sensors Based on PVDF with Sprayed and Transparent Electrodes for Self-Powered Wireless Sensor Nodes." *IEEE Sensors Journal* 19 (3): 1114–26.

Chen, Z., Z. Li, J. Li, C. Liu, C. Lao, Y. Fu, C. Liu, Y. Li, P. Wang, and Y. He. 2019. "3D Printing of Ceramics: A Review." *Journal of the European Ceramic Society* 39 (4): 661–87.

Choy, K. 2003. "Chemical Vapour Deposition of Coatings." *Progress in Materials Science* 48 (2): 57–170.

Das-Gupta, D. K., and K. Doughty. 1978. "Corona Charging and the Piezoelectric Effect in Polyvinylidene Fluoride." *Journal of Applied Physics* 49 (8): 4601–3.

Derraz, M., E. Sabani, C. Ennawaoui, E. M. Loualid, E. M. Laadissi, A. Balhamri, A. Hajjaji, and A. E. Azim. 2022. "Morphological and Ferroelectric Characterizations of Porous Poly (Ethylene-co-vinyl Acetate) Copolymer Films Prepared by Coextrusion and Pressing Methods for Pseudo-piezoelectric Effect." *Materials Today Proceedings* 66: 196–201.

De Vries, D. 2009. "Characterization of Polymeric Foams." *Eindhoven Universitatis Technology* 34.

Dineva, P., D. Gross, R. Müller, and T. Rangelov. 2014. "Piezoelectric Materials." In *Dynamic Fracture of Piezoelectric Materials: Solution of Time-Harmonic Problems via BIEM. Solid Mechanics and Its Applications*, 7–32. Cham: Springer International Publishing.

Dobkin, B. H., and A. Dorsch. 2011. "The Promise of MHealth: Daily Activity Monitoring and Outcome Assessments by Wearable Sensors." *Neurorehabilitation and Neural Repair* 25 (9): 788–98.

Duda, T., and L. V. Raghavan. 2016. "3D Metal Printing Technology." *IFAC-PapersOnLine* 49 (29): 103–10.

Dzifčáková, E., and J. Dudík. 2017. "Chapter 13 - Kappa Distributions and the Solar Spectra: Theory and Observations." In *Kappa Distributions*, edited by G. Livadiotis, 523–47. Elsevier.

Ennawaoui, C., A. Hajjaji, A. Azim, and Y. Boughaleb. 2016. "Theoretical Modeling of Power Harvested by Piezo-Cellular Polymers." *Molecular Crystals and Liquid Crystals* 628 (1): 49–54.

Ennawaoui, C., H. Lifi, A. Hajjaji, C. Samuel, M. Rguiti, S. Touhtouh, A. Azim, and C. Courtois. 2019. "Dielectric and Mechanical Optimization Properties of Porous Poly(Ethylene- *Co* -vinyl Acetate) Copolymer Films for Pseudo-piezoelectric Effect." *Polymer Engineering and Science* 59 (7): 1455–61.

Ennawaoui, C., A. Hajjaji, C. Samuel, E. Sabani, A. Rjafallah, I. Najihi, E. M. Laadissi, E. M. Loualid, M. Rguiti, A. E. Ballouti, and A. Azim. 2021. "Piezoelectric and Electromechanical Characteristics of Porous Poly(Ethylene-Co-Vinyl Acetate) Copolymer Films for Smart Sensors and Mechanical Energy Harvesting Applications." *Applied Systems Innovation* 4 (3): 57.

Fangachi, N., I. Najihi, M. Yessari, and A. Hajjaji. 2022. "Energy Harvesting Using a Dynamic Weighing System Based on Piezoelectric Materials." *The European Physical Journal - Applied Physics* 97, https://doi.org/10.1051/epjap/2022220100.

Fang, P., M. Wegener, W. Wirges, R. Gerhard, and L. Zirkel. 2007. "Cellular Polyethylene-Naphthalate Ferroelectrets: Foaming in Supercritical Carbon Dioxide, Structural and Electrical Preparation, and Resulting Piezoelectricity." *Applied Physics Letters* 90 (19): 192908.

Fang, P., Y. Peng, W.-H. Lin, Y. Wang, S. Wang, X. Zhang, K. Wu, and G. Li. 2021. "Wrist Pulse Recording with a Wearable Piezoresistor-Piezoelectric Compound Sensing System and its Applications in Health Monitoring." *IEEE Sensors Journal* 21 (18): 20921–30.

Falconi, D. R., R. A. C. Altafim, R. A. P. Altafim, H. C. Basso, W. Wirges, and R. Gerhard. 2010. "Piezoelectric Sensor Based on Electret Thermoforming Technology." In *2010 10th IEEE International Conference on Solid Dielectrics*, 1–3.

Gerhard-Multhaupt, R. 2002. " Less Can Be More Holes in Polymers Lead to a New Paradigm of Piezoelectric Materials for Electret Transducers." *IEEE Transactions on Dielectrics and Electrical Insulation* 9 (5): 850–9.

Gerhard-Multhaupt, R., M. Wegener, W. Wirges, J. A. Giacometti, R. C. Altafim, L. F. Santos, R. M. Faria, and M. Paajanen. 2002. "Electrode Poling of Cellular Polypropylene Films with Short High-Voltage Pulses." In *Annual Report Conference on Electrical Insulation and Dielectric Phenomena*, 299–302. Cancun: IEEE.

González-Losada, P., H. Yang, R. M. R. Pinto, M. Faraji, R. Dias, and K. Vinayakumar 2022. "Flexible Ferroelectret for Zero Power Wearable Application." In *2022 IEEE International Conference on Flexible and Printable Sensors and Systems (FLEPS)*, 1–4.

Hall, A., M. Allahverdi, E. K. Akdogan, and A. Safari. 2005. "Piezoelectric/Electrostrictive Multimaterial PMN-PT Monomorph Actuators." *Journal of the European Ceramic Society* 25 (12): 2991–7.

Ham, S. S., G.-J. Lee, D. Y. Hyeon, Y. Kim, Y. Lim, M.-K. Lee, J.-J. Park, G.-T. Hwang, S. Yi, C. K. Jeong, and K.-I. Park. 2021. "Kinetic Motion Sensors Based on Flexible and Lead-Free Hybrid Piezoelectric Composite Energy Harvesters with Nanowires-Embedded Electrodes for Detecting Articular Movements." *Composites Part B: Engineering* 212: 108705.

Hamdi, O., F. Mighri, and D. Rodrigue. 2018. "Department of Chemical Engineering, Université Laval, Quebec, G1V0A6, Canada. Piezoelectric Cellular Polymer Films: Fabrication, Properties and Applications." *AIMS Materials Science* 5 (5): 845–69.

Han, X., C. Zeng, L. J. Lee, K. W. Koelling, and D. L. Tomasko. 2003. "Extrusion of Polystyrene Nanocomposite Foams with Supercritical CO2." *Polymer Engineering and Science* 43 (6): 1261–75.

Heck, R. L. 1998. "A Review of Commercially Used Chemical Foaming Agents for Thermoplastic Foams." *Journal of Vinyl and Additive Technology* 4 (2): 113–6.

Hillenbrand, J., and G. M. Sessler. 2004. "Quasistatic and Dynamic Piezoelectric Coefficients of Polymer Foams and Polymer Film Systems." *IEEE Transactions on Dielectrics and Electrical Insulation* 11 (1): 72–9.

Hillenbrand, J., N. Behrendt, V. Altstädt, H.-W. Schmidt, and G. M. Sessler. 2006. "Electret Properties of Biaxially Stretched Polypropylene Films Containing Various Additives." *Journal of Physics D: Applied Physics* 39 (3): 535–40.

Hillenbrand, J., P. Pondrom, and G. M. Sessler. 2015. "Electret Transducer for Vibration-Based Energy Harvesting." *Applied Physics Letters* 106 (18): 183902.

Japon, S., Y. Leterrier, and J.-A. E. Månson. 2000. "Recycling of Poly(Ethylene Terephthalate) into Closed-Cell Foams: Recycling of PET into Closed-Cell Foams." *Polymer Engineering and Science* 40 (8): 1942–52.

Jarrasse, N., C. Nicol, A. Touillet, F. Richer, N. Martinet, J. Paysant, and J. B. de Graaf. 2017. "Classification of Phantom Finger, Hand, Wrist, and Elbow Voluntary Gestures in Transhumeral Amputees with SEMG." *IEEE Transactions on Neural Systems and Rehabilitation Engineering* 25 (1): 71–80.

Jiao, P., Y. Yang, K. I. Egbe, Z. He, and Y. Lin. 2021. "Mechanical Metamaterials Gyro-Structure Piezoelectric Nanogenerators for Energy Harvesting under Quasi-Static Excitations in Ocean Engineering." *ACS Omega* 13. https://doi.org/10.1021/acsomega.1c01687.

Kacprzyk, R. 2017. "Piezoelectric Properties of Non-uniform Polymeric Structures under Static Load." *Phase Transitions* 90 (1): 104–11.

Kaczmarek, H., B. Królikowski, M. Chylińska, E. Klimiec, and D. Bajer. 2019. "Piezoelectric Films Based on Polyethylene Modified by Aluminosilicate Filler." *Polymers* 11 (8): 1345.

Kierzewski, I., S. S. Bedair, B. Hanrahan, H. Tsang, L. Hu, and N. Lazarus. 2020. "Adding an Electroactive Response to 3D Printed Materials: Printing a Piezoelectric." *Additive Manufacturing* 31: 100963.

Klimiec, E., H. Kaczmarek, B. Królikowski, and G. Kołaszczyński. 2020. "Cellular Polyolefin Composites as Piezoelectric Materials: Properties and Applications." *Polymers* 12 (11): 2698.

Klimiec, E., H. Kaczmarek, B. Królikowski, and G. Kołaszczyński. 2020. "Cellular Polyolefin Composites as Piezoelectric Materials: Properties and Applications." *Polymers* 12 (11): 2698.

Koenig, J. L. 1999. "Chapter 10 - Mass Spectrometry of Polymers." In *Spectroscopy of Polymers*, 2nd ed. edited by J. L. Koenig, 441–80. New York: Elsevier Science.

Kong, Y., and J. N. Hay. 2002. "The Measurement of the Crystallinity of Polymers by DSC." *Polymer* 43 (14): 3873–8.

Konstantinidis, I.C., G. Paradisiadis, and D. N. Tsipas. 2009. "Analytical Models for the Mechanical Behavior of Closed and Open-Cell Al Foams." *Theoretical and Applied Fracture Mechanics* 51 (1): 48–56.

Lai, Z., T. Zhao, P. Zhu, J. Xiang, D. Liu, X. Liang, and R. Sun. 2021. "Rapid Metallization by Copper Electroplating on Insulating Substrate Using Silver Nanowires Conductive Composite as Seed Layer." *Composites Communications* 27: 100819.

Lanceros-Méndez, S., and P. Martins. 2017. *Magnetoelectric Polymer-Based Composites: Fundamentals and Applications*. New York: John Wiley & Sons.

Lee, S.-T., and C. B. Park. 2014. *Foam Extrusion: Principles and Practice*, 2nd ed. Boca Raton: CRC Press.

Licari, J. J., and D. W. Swanson. 2011. "Chapter 7 - Test and Inspection Methods." In *Adhesives Technology for Electronic Applications. Materials and Processes for Electronic Applications*, 2nd ed. edited by J. J. Licari, and D. W. Swanson, 345–77. Oxford: William Andrew Publishing.

Li, W., N. Wu, J. Zhong, Q. Zhong, S. Zhao, B. Wang, X. Cheng, S. Li, K. Liu, B. Hu, and J. Zhou. 2016. "Theoretical Study of Cellular Piezoelectric Generators." *Advances in Functional Materials* 26 (12): 1964–74.

Lifshitz, C., and T. D. Märk. 1999. "Ionization Theory." In *Encyclopedia of Spectroscopy and Spectrometry*, edited by J. C. Lindon, 1010–21. Oxford: Elsevier.

Lopes, A. C., C. M. Costa, C. J. Tavares, I. C. Neves, and S. Lanceros-Mendez. 2011. "Nucleation of the Electroactive γ Phase and Enhancement of the Optical Transparency in Low Filler Content Poly(Vinylidene)/Clay Nanocomposites." *Journal of Physical Chemistry C* 115 (37): 18076–82.

Mahadeva, S. K., J. Berring, K. Walus, and B. Stoeber. 2013. "Effect of Poling Time and Grid Voltage on Phase Transition and Piezoelectricity of Poly(Vinyledene Fluoride) Thin Films Using Corona Poling." *Journal of Physics D: Applied Physics* 46 (28): 285305.

Malki, Z., C. Ennawaoui, A. Hajjaji, I. Najihi, M. Eljouad, and Y. Boughaleb. 2020. "Pedestrian Crossing System for the Mechanical Energy Harvesting Using Piezoelectric Materials." *IOP Conference Series: Materials Science and Engineering* 948 (1): 012030.

Martin, P. M. 2010. "Surface Preparation for Film and Coating Deposition Processes." In *Handbook of Deposition Technologies for Films and Coatings*, 93–134. Norwich, NY: William Andrew Publishing.

Martín-Palma, R. J., and A. Lakhtakia. 2013. "Vapor-Deposition Techniques." In *Engineered Biomimicry*, 383–98. United States: Elsevier.

Mason, W. P. 1981. "Piezoelectricity, its History and Applications." *Journal of the Acoustical Society of America* 70 (6): 1561–6.

Moghadam, M. Z., Sh. Hassanajili, F. Esmaeilzadeh, M. Ayatollahi, and M. Ahmadi. 2017. "Formation of Porous HPCL/LPCL/HA Scaffolds with Supercritical CO2 Gas Foaming Method." *Journal of the Mechanical Behavior of Biomedical Materials* 69: 115–27.

Najihi, I., C. Ennawaoui, A. Hajjaji, and Y. Boughaleb. 2022. "3D Printed Cellular Piezoelectric Polymers for Smart Sensors/Autonomous Energy Harvesters." *Materials Today Proceedings*. https://doi.org/10.1016/j.matpr.2022.06.203.

Najihi, I., C. Ennawaoui, A. Hajjaji, and Y. Boughaleb. 2021. "Theoretical Modeling of Longitudinal Piezoelectric Characteristic for Cellular Polymers." *Cellular Polymers* 41: 39–50.

Nie, J., M. Ji, Y. Chu, X. Meng, Y. Wang, J. Zhong, and L. Lin. 2019. "Human Pulses Reveal Health Conditions by a Piezoelectric Sensor via the Approximate Entropy Analysis." *Nano Energy* 58: 528–35.

Nykänen, H., M. Antila, J. Kataja, J. Lekkala, and S. Uosukainen. 1999. "Active Control of Sound Based on Utilizing EMFI-Technology: International Symposium on Active Control of Sound and Vibration, ACTIVE 99." *INTER-NOISE NOISE-CON Congress Conference Proceeding Acta* 1159–70.

Paajanen, M., H. Valimaki, and J. Lekkala. 1999. "Modelling the Sensor and Actuator Operations of the ElectroMechanical Film EMFi." In *10th International Symposium on Electrets (ISE 10).* Proceedings (Cat. No. 99 CH36256), 735–8. IEEE.

Palito, T., R. Altafim, Y. Olivato, and J. Carmo. 2019. "Hydrophone Based on 3D Printed Polypropylene (PP) Piezoelectric." *Electronics Letters* 55: 203–4.

Palitó, T. T. C., Y. A. O. Assagra, R. A. P. Altafim, J. P. Carmo, and R. A. C. Altafim. 2019. "Hydrophone Based on 3D Printed Polypropylene (PP) Piezoelectric." *Electronics Letters* 55 (4): 203–4.

Paschen, F. 1889. "Ueber die zum Funkenübergang in Luft, Wasserstoff und Kohlensäure bei verschiedenen Drucken erforderliche Potentialdifferenz." *Annales de Physique* 273 (5): 69–96.

Qaiss, A., and M. Bousmina. 2011. "Biaxial Stretching of Polymers Using a Novel and Versatile Stretching System." *Polymer Engineering and Science* 51 (7): 1347–53.

Qaiss, A., H. Saidi, O. Fassi-Fehri, and M. Bousmina. 2012. "Cellular Polypropylene-Based Piezoelectric Films." *Polymer Engineering and Science* 52 (12): 2637–44.

Qaiss, A., H. Saidi, O. Fassi-Fehri, and M. Bousmina. 2013. "Theoretical Modeling and Experiments on the Piezoelectric Coefficient in Cellular Polymer Films." *Polymer Engineering and Science* 53 (1): 105–11.

Qiu, X. 2010. "Patterned Piezo-, Pyro-, and Ferroelectricity of Poled Polymer Electrets." *Journal of Applied Physics* 108 (1): 011101.

Ramadan, K. S., D. Sameoto, and S. Evoy. 2014. "A Review of Piezoelectric Polymers as Functional Materials for Electromechanical Transducers." *Smart Materials and Structures* 23 (3): 033001.

Rupitsch, S. J. 2019. "Piezoelectric Sensors and Actuators." *Simulation Piezoelectric Sensing Actuator Devices Piezoelectric Sensing Actuators Topography Mining Metallurgical Materials Engineering*: 83–126.

Rupitsch, S., R. Lerch, J. Strobel, and A. Streicher. 2011. "Ultrasound Transducers Based on Ferroelectret Materials." *IEEE Transactions on Dielectrics and Electrical Insulation* 18 (1): 69–80.

Samadi, A., R. Hasanzadeh, T. Azdast, H. Abdollahi, P. Zarrintaj, and M. R. Saeb. 2020. "Piezoelectric Performance of Microcellular Polypropylene Foams Fabricated Using Foam Injection Molding as a Potential Scaffold for Bone Tissue Engineering." *Journal of Macromolecular Science Part B* 59 (6): 376–89.

Senturia, S. D. 2007. *Microsystem Design*. United states: Springer Science & Business Media.

Sessler, G. M., and J. Hillenbrand. 1999. "Electromechanical Response of Cellular Electret Films." *Applied Physics Letters* 75 (21): 3405–7.

Setter, N., D. Damjanovic, L. Eng, G. Fox, S. Gevorgian, S. Hong, A. Kingon, H. Kohlstedt, N. Y. Park, G. B. Stephenson, I. Stolitchnov, A. K. Taganstev, D. V. Taylor, T. Yamada, and S. Streiffer. 2006. "Ferroelectric Thin Films: Review of Materials, Properties, and Applications." *Journal of Applied Physics* 100 (5): 051606.

Sherrit, S., N. Gauthier, H. D. Wiederick, B. K. Mukherjee, and S. E. Prasad. 1991. "The Effect of Electrode Materials on Measured Piezoelectric Properties of Ceramics and Ceramic-Polymer Composites." In *[Proceedings] 1990 IEEE 7th International Symposium on Applications of Ferroelectrics*, 346–9. Urbana: IEEE.

Song, H.-C., P. Kumar, D. Maurya, M.-G. Kang, W. T. Reynolds, D.-Y. Jeong, C.-Y. Kang, and S. Priya. 2017. "Ultra-Low Resonant Piezoelectric MEMS Energy Harvester with High Power Density." *Journal of Microelectromechanical Systems* 26 (6): 1226–34.

Sotgiu, E., P. González-Losada, R. M. R. Pinto, H. Yang, M. Faraji, and K. B. Vinayakumar. 2022. "Pyroelectrically Charged Flexible Ferroelectret-Based Tactile Sensor for Surface Texture Detection." *Electronics* 11 (15): 2329.

Stevenson, P. 2010. "Inter-Bubble Gas Diffusion in Liquid Foam." *Current Opinion in Colloid and Interface Science* 15 (5): 374–81.

Šutka, A., K. Mālnieks, A. Linarts, M. Timusk, V. Jurķāns, I. Gorņevs, J. Blūms, A. Bērziņa, U. Joost, and M. Knite. 2018. "Inversely Polarised Ferroelectric Polymer Contact Electrodes for Triboelectric-like Generators from Identical Materials." *Energy and Environmental Science* 11 (6): 1437–43.

Swann, S. 1988. "Magnetron Sputtering." *Physics in Technology* 19 (2): 67–75.

Townsend, J. S. 1915. *Electricity in Gases*. Oxford: Рипол Классик.

Wang, X., M. Jiang, Z. Zhou, J. Gou, and D. Hui. 2017. "3D Printing of Polymer Matrix Composites: A Review and Prospective." *Composites Part B: Engineering* 110: 442–58.

Wang, X., S. Hu, Y. Guo, G. Li, and R. Xu. 2019. "Toughened High-Flow Polypropylene with Polyolefin-Based Elastomers." *Polymers* 11 (12): 1976.

Wang, H.; Li, Y.; Wang, X.; Liu, Z.; Ahmed, M. F.; Zeng, C. 2021. "Preparation and Characterization of Piezoelectric Foams Based on Cyclic Olefin Copolymer." *Engineering and Science* 16: 203–10.

Wang, N., R. Daniels, L. Connelly, M. Sotzing, C. Wu, R. Gerhard, G. A. Sotzing, and Y. Cao. 2021. "All-Organic Flexible Ferroelectret Nanogenerator with Fabric-Based Electrodes for Self-Powered Body Area Networks." *Small* 17 (33): 2103161.

Warfield, R. W., and M. C. Petree. 1961. "Electrical Resistivity of Polymers." *Polymer Engineering and Science* 1 (2): 80–5.

Wegener, M., W. Wirges, J. Fohlmeister, B. Tiersch, and R. Gerhard-Multhaupt. 2004. "Two-Step Inflation of Cellular Polypropylene Films: Void-Thickness Increase and Enhanced Electromechanical Properties." *Journal of Physics D: Applied Physics* 37 (4): 623–7.

Wieser, M. E., and W. A. Brand. 1999. "Isotope Ratio Studies Using Mass Spectrometry." In *Encyclopedia of Spectroscopy and Spectrometry*, edited by J. C. Lindon, 1072–86. Oxford: Elsevier.

Wirges, W., M. Wegener, O. Voronina, L. Zirkel, and R. Gerhard-Multhaupt. 2007. "Optimized Preparation of Elastically Soft, Highly Piezoelectric, Cellular Ferroelectrets from Nonvoided Poly(Ethylene Terephthalate) Films." *Advances in Functional Materials* 17 (2): 324–9.

Won, S. S., M. Kawahara, C. W. Ahn, J. Lee, J. Lee, C. K. Jeong, A. I. Kingon, and S.-H. Kim. 2020. "Lead-free Bi0.5(Na0.78K0.22)TiO3 Nanoparticle Filler–Elastomeric Composite Films for Paper-Based Flexible Power Generators." *Advanced Electronics Materials* 6 (2): 1900950.

Wu, N., X. Cheng, Q. Zhong, J. Zhong, W. Li, B. Wang, B. Hu, and J. Zhou. 2015. "Cellular Polypropylene Piezoelectric for Human Body Energy Harvesting and Health Monitoring." *Advances in Functional Materials* 25 (30): 4788–94.

Yan, X., G. Liu, M. Dickey, and C. G. Willson. 2004. "Preparation of Porous Polymer Membranes Using Nano- or Micro-pillar Arrays as Templates." *Polymer* 45 (25): 8469–74.

Yasuda, H., and C. E. Lamaze. 1973. "Polymerization in an Electrodeless Glow Discharge. II. Olefinic Monomers." *Journal of Applied Polymer Science* 17 (5): 1519–31.

Zhang, X., J. Hillenbrand, and G. M. Sessler. 2007. "Ferroelectrets with Improved Thermal Stability Made from Fused Fluorocarbon Layers." *Journal of Applied Physics* 101 (5): 054114.

Zhang, X., J. Hillenbrand, and G. M. Sessler. 2006. "Thermally Stable Fluorocarbon Ferroelectrets with High Piezoelectric Coefficient." *Applied Physics A: Solids and Surfaces* 84 (1–2): 139–42.

Zhong, Q., J. Zhong, X. Cheng, X. Yao, B. Wang, W. Li, N. Wu, K. Liu, B. Hu, and J. Zhou. 2015. "Paper-Based Active Tactile Sensor Array." *Advances in Materials* 27 (44): 7130–6.

Zhong, J., Q. Zhong, X. Zang, N. Wu, W. Li, Y. Chu, and L. Lin. 2017. "Flexible PET/EVA-Based Piezoelectric Generator for Energy Harvesting in Harsh Environments." *Nano Energy* 37: 268–74.

Zhukov, S., D. Eder-Goy, S. Fedosov, B.-X. Xu, and H. von Seggern. 2018. "Analytical Prediction of the Piezoelectric D33 Response of Fluoropolymer Arrays with Tubular Air Channels." *Scientific Reports* 8 (1): 4597.

Zuo, X., L. Chen, W. Pan, X. Ma, T. Yang, and X. Zhang. 2020. "Fluorinated Polyethylene Propylene Ferroelectrets with an Air-Filled Concentric Tunnel Structure: Preparation, Characterization, and Application in Energy Harvesting." *Micromachines* 11 (12): 1072.